Journal of Nuclear Materials 557 (2021) 153312

Contents lists available at ScienceDirect

Journal of Nuclear Materials

journal homepage: www.elsevier.com/locate/jnucmat

Modelling of thermal conductivity and melting behaviour of minor actinide-MOX fuels and assessment against experimental and molecular dynamics data

A. Magni[a], L. Luzzi[a], D. Pizzocri[a], A. Schubert[b], P. Van Uffelen[b], A. Del Nevo[c,*]

[a] Politecnico di Milano, Department of Energy, Nuclear Engineering Division, via La Masa 34, 20156, Milano, Italy
[b] European Commission, Joint Research Centre (JRC), Karlsruhe, Germany
[c] ENEA, FSN-ING-SIS, CR Brasimone, 40032, Camugnano (BO), Italy

ARTICLE INFO

Article history:
Received 10 June 2021
Revised 6 September 2021
Accepted 22 September 2021
Available online 24 September 2021

Keywords:
Nuclear fuel
Minor actinide-bearing MOX
Thermal conductivity
Melting temperature
Modelling and assessment

ABSTRACT

Recycling and burning minor actinides (MA, e.g., americium, neptunium) in mixed-oxide (MOX) nuclear fuel is a strategic option for fast reactor concepts of Generation IV, especially considering the current interest in the ultimate radioactive waste management and sustainability improvement by better use of natural resources. Among the fuel properties, thermal conductivity and melting temperature are pivotal since they determine, respectively, the fuel temperature profile and the fundamental safety limit on the margin to fuel melting, hence impacting on the overall fuel performance under irradiation and allowing the safe irradiation of the fuel pin. Nevertheless, the available literature about Am- or Np-containing MOX is currently scarce, both regarding experimental data and models. Moreover, state-of-the-art fuel performance codes (FPCs, e.g., TRANSURANUS) do not account for the effects of minor actinides on MOX fuel properties. This work presents original correlations for thermal conductivity and melting temperature of minor actinide-MOX fuels, i.e., (U, Pu, Am, Np)O_{2-x}, derived based on the available literature and accessible data, which are herein extensively reviewed. The assessment of the novel correlations is first performed in a statistical way, evaluating the regressor p-values which indicate their significance with respect to the available experimental dataset used for the fitting procedure. Additionally, the novel correlations for MA-MOX are assessed against both measured and calculated data (from Molecular Dynamics simulations), yielding an accuracy in line with the already existing correlations and with the state-of-the-art experimental uncertainties. Finally, the potential integral impact of a homogeneous minor actinide content in the fuel is illustrated on the basis of a fuel pin fast-ramped up to fuel melting during the HEDL P-19 irradiation experiment.

Introduction

The development of Generation IV nuclear reactor concepts foresees the utilization of mixed-oxide uranium-plutonium fuel (MOX) to be irradiated under fast neutron flux [1,2]. Another option is represented by the adoption of Minor Actinide-bearing MOX (MA-MOX, i.e., (U, Pu, MA)O_{2-x}), with the aim of recycling and burning minor actinides (americium, neptunium) as a strategic choice for a better management of ultimate radioactive waste and the improvement of the sustainability of Generation IV fast reactor systems by a broader exploitation of fuel resources. Two strategies exist for the fabrication and exploitation of MA-MOX fuels, i.e., the homogeneous one, corresponding to low minor actinide contents in the pellets (typically around 2–3 wt.%, up to 5 wt.%) [3], and the heterogeneous one, consisting in higher minor actinide contents of ~ 10–15 wt.% [3–5]. The investigation of thermal properties of homogeneous MA-MOX fuels has started in the framework of the INSPYRE H2020 Project [6,7] and both homogeneous and heterogeneous MA-MOX fuel concepts are of interest and under consideration (as driver and blanket fuels, respectively) for application in the MYRRHA Gen-IV reactor concept [8–10], in the framework of the PATRICIA H2020 Project [11]. PATRICIA is indeed devoted to feasibility studies of the transmutation of minor actinides (americium, especially) in fuel pellets under irradiation in the MYRRHA facility.

* Corresponding author.
E-mail address: alessandro.delnevo@enea.it (A.D. Nevo).

https://doi.org/10.1016/j.jnucmat.2021.153312

Since the margin to fuel melting is one of the main design limits for the safe operation of fuel pins, ensuring the integrity of the fuel pellets under irradiation, analysing the thermal performance of nuclear fuel is of fundamental importance, especially in fast reactor environments (characterized by harsh irradiation conditions, e.g., higher linear heat rates with respect to light water reactors, higher expected fuel burn-up [12,13]). Additionally, when MOX fuel is irradiated to the target high burn-up for Gen-IV applications [1,2], significant quantities of fission products and minor actinides will exist in the fuel matrix, in solid solution and as precipitations of oxide or metallic inclusions. In principle, this fuel microstructure modification during irradiation directly affects the fuel thermal and mechanical properties. Hence, the impact of the minor actinide content on the evolution of MOX fuel properties needs evaluation and assessment. In this work, the focus is on the thermal conductivity and melting (solidus) temperature properties of Am- and Np-bearing MOX fuels, fundamental (as for any other kind of nuclear fuel) since determining the fuel temperature profile and the melting safety margin, respectively, and impacting on the overall fuel performance under irradiation.

In spite of the strong interest in the recycling and burning of minor actinides (MA-MOX fuels are currently major candidates as advanced nuclear fuels to be employed in fast breeder and transmutation reactors [12–14]), measurements of physical properties of MA-MOX fuels are scarcely reported in the state-of-the-art literature. This is mainly due to the limited amount of MA resources and to the difficulties in fabricating and measuring materials containing highly radioactive MA isotopes (e.g., Am-241, α-decaying). Therefore, Molecular Dynamics (MD) can be a useful simulation technique to obtain information on the behaviour of MA-containing materials and to evaluate their physical properties on a lower-length scale basis (see e.g., a recent work on molecular dynamics calculations on different types of nuclear fuels [15]). This contributes to the development and implementation in fuel performance codes (FPCs, e.g., TRANSURANUS [16–18]) of suitable models for the MA-MOX properties, accounting for the minor actinide effects in an assessed way.

This work presents novel correlations for the thermal conductivity and melting temperature of minor actinide-MOX fuel, i.e., (U, Pu, Am, Np)O_{2-x}, which have been derived based on available and accessible literature data, and assessed for what concerns the terms related to the minor actinide contents. Indeed, the correlations herein proposed extend previous ones developed for fast reactor U-Pu MOX fuels by the same authors [19], keeping the same comprehensive set of dependencies and adding the ones on the minor actinides Am and Np (covering the homogeneous MA-MOX strategy and the heterogeneous one as much as possible, in terms of ranges of applicability). The correlation regressors related to the minor actinide contents are first statistically assessed based on the respective p-values, to evaluate their significance with respect to the available experimental dataset, and then derived from a best fit of the data. The novel correlations for MA-MOX are assessed against both measured and calculated data (from molecular dynamics simulations). The ultimate aim is to overcome the current limitations of the modelling of the thermal properties of MOX fuels in fuel performance codes, towards their extension to fast reactor conditions and application to safety analyses on Generation IV reactor concepts. Indeed, as an illustrative example, the herein proposed correlations for MA-MOX are employed to simulate the thermal performance of a fast reactor fuel pin chosen from the HEDL P-19 database [20]. HEDL P-19 was a power-to-melt experiment performed on U-Pu MOX fuel and already considered for validation of the MOX thermal property correlations previously developed by the same authors [19]. In this work, the potential impact of a 5 at.% Am content in the HEDL P-19 fuel is evaluated, in terms of fuel central temperature evolution, fuel-cladding radial gap width and fuel restructuring, comparing the integral pin performance results (as predicted by the TRANSURANUS fuel performance code [16,21]) to those obtained for U-Pu MOX under the same experimental HEDL P-19 irradiation conditions, i.e., fast power ramps up to fuel melting.

The paper is organized as follows. An extensive overview of the currently available state-of-the-art, concerning both thermal conductivity and melting temperature of minor actinide-bearing MOX and including both experimental and molecular dynamics data, is provided in Section 2. As a complement, the already existing correlations for both thermal properties are recalled and presented in Section 3. Sections 4 and 5 present the development and assessment of the novel, comprehensive correlations for the thermal conductivity and melting temperature of MA-MOX, respectively, showing the accuracy of the correlation predictions compared to the state-of-the-art literature correlations. The application of the novel correlations in the TRANSURANUS code to a test case, i.e., the thermal performance of a fast reactor fuel pin irradiated up to fuel melting, is illustrated in Section 6. Conclusions are drawn in Section 7.

State-of-the-art experimental and Molecular Dynamics data

The majority of experimental and simulation activities on MA-MOX (mainly Am-bearing) started in the '90s, along with the development of Gen-IV fast reactor concepts and the related interest in the possibility of minor actinide transmutation. Although some experimental campaigns on minor actinide (Am, Np)-bearing fuels were performed earlier (e.g., the SUPERFACT-1 irradiation experiment [3]), the available open literature works date back to 20 years ago at the most, as reported by the following Tables 1 and 2. These tables provide a comprehensive collection of all the literature works about MA-MOX thermal conductivity and melting temperature currently available to the authors.

Concerning the MA-MOX thermal conductivity, the experimental measurements as a function of temperature prove to be well described by the classical solid-state physically-grounded formula, i.e., including the lattice vibration contribution (dominating at low temperatures and representing the phonon–phonon interaction (Umklapp process) and the density of defects in the lattice) and the contribution from free electrons (dominating at high temperatures) [22,23]. Indeed, the measured MA-MOX thermal conductivity according to the present knowledge decreases with increasing temperature (down to a minimum value at around 1800–2000 K) [23–26], while a slight increase of the conductivity at higher temperatures is indicated by MD calculations [27,28] and measurements on U-Pu MOX fuels [19,29,30]. This kind of behaviour holds for any value (in reasonable ranges) of fuel deviation from stoichiometry (corresponding to an oxygen-to-metal ratio O/M = 2.00), porosity and minor actinide (Am, Np) contents, as shown e.g. by [24–26].

The effect of the plutonium content and the degradation of the thermal conductivity with increasing burn-up (during fuel irradiation) is suggested by observations on U-Pu MOX rather than on MA-MOX. Indeed, the available references (Table 1) mostly analyse the effect of MAs for a fixed Pu content, while only one author provides two experimental data on irradiated MA-MOX [22], which is not sufficient to derive a burn-up effect specifically representative of MA-MOX.

A clear and quantitative indication of the small effect of the MA content on the fuel thermal conductivity is provided by the experimental data of Kato et al., [22]. It is reported that the Np and Am additions to MOX caused the measured data to slightly decrease (in the low temperature range < 1000 K), i.e., the 1.6 at.% Am and 1.6 at.% Np contents therein analysed caused the thermal conductivity to decrease by 2.0–2.5% of the corresponding U-Pu MOX

Table 1
List of references of MA-MOX thermal conductivity experimental and molecular dynamics (MD) data, detailing the fuel material and the experimental/calculation technique employed.

Reference	Measured/simulated fuel	Experimental/calculation technique
Kurosaki et al. [27]	MD calculations on fresh, stoichiometric Am-MOX: $(U_{0.7-z}\ Pu_{0.3}\ Am_z)O_2$, z = 0, 0.016, 0.03, 0.05, 0.1, 0.15. T = 300 - 2500 K, density = 100% TD (Theoretical Density).	Ions initially arranged in a CaF_2-type crystal structure. Calculations performed using a MD program based on MXDORTO, employing the semi-empirical two-body potential function by Ida [41]. Thermal conductivity calculated using the Green-Kubo relation.
Morimoto et al. [24]	Fresh, stoichiometric Am-MOX: $(U_{0.7-z}\ Pu_{0.3}\ Am_z)O_2$, z = 0.007, 0.022, 0.03. T = 873 - 1673 K, density = 84.3% - 100% TD.	Laser-flash method for the simultaneous measurement of thermal diffusivity and specific heat capacity (with a calorimeter in the sample position).
Morimoto et al. [25]	Fresh, hypo-stoichiometric Am-MOX: $(U_{0.678}\ Pu_{0.3}\ Am_{0.022})O_{2-x}$, x = 0.001 - 0.085. T = 870 - 1773 K, density = 100% TD.	Laser-flash method for the simultaneous measurement of thermal diffusivity and specific heat capacity (with a calorimeter in the sample position).
Morimoto et al., 2009 [26]	Fresh, stoichiometric Np-MOX: $(U_{0.7-z}\ Pu_{0.3}\ Np_w)O_2$, w = 0.06, 0.12. T = 870 - 1800 K, density = 93%, 94.1% TD.	Laser-flash method for the simultaneous measurement of thermal diffusivity and specific heat capacity (with a calorimeter in the sample position).
Kato et al. [22]	Irradiated, hypo-stoichiometric MA-MOX: $(U_{0.668}\ Pu_{0.3}\ Np_{0.016}\ Am_{0.016})O_{2-x}$, x = 0.017, 0.043. T = 1273 K, density = 93% TD, burn-up = 0.082 GWd/t_{HM}.	Short irradiation tests performed in the fast reactor Joyo [42–45]. Thermal conductivity evaluated from irradiated samples characteristics, according to correlations from [24–26].
Prieur et al. [23]	Fresh, hypo-stoichiometric MA-MOX: $(U_{0.74}\ Pu_{0.22}\ Am_z\ Np_w)O_{2-x}$, (x, z, w) = (0.01, 0.02, 0.02) and (0.02, 0.035, 0.005). T = 540 - 1615 K, density = 94.8%, 94.6% TD.	Thermal diffusivity measurement: shielded laser-flash device, temperature perturbation on the opposite surface of the sample recorded with a pyrometer. Thermal conductivity calculated via heat capacity (Neumann-Kopp's law) and density (from measured lattice parameter, accounting for porosity).
Li et al.[28]	MD calculations on fresh, stoichiometric Am-MOX: $(U_{0.7-z}\ Pu_{0.3}\ Am_z)O_2$, z = 0, 0.03, 0.05, 0.1, 0.15, 0.2, 0.25. T = 500 - 3000 K, density = 100% TD.	EMD simulations with LAMMPS program, on 3 different fluorite unit cells: 4 × 4 × 4, 5 × 5 × 5 and 8 × 8 × 8 unit cells. BMH interatomic potential, with PIM. Thermal conductivity calculated according to Green-Kubo relation.
Yokohama et al. [46]	Fresh, stoichiometric Am-MOX: Pu content = 30 at.%, Am content = 10 at.%, T = 300 - 1500 K, density = 100% TD.	Thermal diffusivity measurement with laser-flash method, after heat treatment at 1473 K (to recover lattice defects induced by self-irradiation during long-term storage, and to adjust the O/M ratio of the sample to 2.00). Thermal conductivity calculated via heat capacity (Kopp's law) and density (measured).

Table 2
List of references for MA-MOX melting temperature experimental and molecular dynamics (MD) data, detailing the fuel material and the experimental/calculation technique employed.

Reference	Measured/simulated fuel	Experimental/calculation technique
Konno et al. [31]	Fresh and irradiated Am-MOX: burn-up = 0 - 124 GWd/t_{HM}, O/M = 1.95 - 1.98, Pu content ~ 30 mol%, Am content = 0.04 and 0.9 mol%.	Thermal arrest technique on samples in W capsules.
Konno et al. [33]	Irradiated Am-MOX: burn-up = 8.2 - 110.9 GWd/t_{HM}, O/M = 1.98 – 1.99, Pu content = 17.5 mol%, Am content = 0.13 mol%.	Thermal arrest technique on sample in a W capsule.
Morimoto et al. [40]	Fresh MA-MOX (Sample 1): $(U_{0.66}\ Pu_{0.30}\ Am_{0.02}\ Np_{0.02})O_{2-x}$, x=0.012, 0.037. Samples 2 and 3: $(U_{0.64}\ Pu_{0.30}\ Am_{0.02}\ Np_{0.02}\ FP_{0.02})O_{2-x}$ (including simulated fission products).	Thermal Arrest technique and analysis of pyrometer thermograms.
Kato et al. [32]	Fresh Am-MOX, O/M = 1.922 - 2.000, Pu content = 11.7 - 60.0 mol%, Am content = 0.3 - 3.3 mol%.	Sample heating in Re or W capsules, analysis of pyrometer thermograms.
Kato et al. [22]	Irradiated, hypo-stoichiometric MA-MOX: $(U_{0.668}\ Pu_{0.3}\ Np_{0.016}\ Am_{0.016})O_{2-x}$, x = 0.017, 0.043, burn-up = 0.082 GWd/t_{HM}.	Short irradiation tests performed in the fast reactor Joyo [42–45]. Samples in Re inner capsule, model for solidus/liquidus temperatures (based on ideal solid solution) employed for interpretation of measurements.
Tanaka et al. [34]	Irradiated Am-MOX fuel containing simulated fission products: $(U_{0.665}\ Pu_{0.29}\ Am_{0.03}\ FP_{0.015})O_2$, burn-up = 150 GWd/$t_{HM}$.	Thermal arrest method on crushed pellet loaded into a Re inner capsule (W outer capsule).
Prieur et al. [23]	Fresh, hypo-stoichiometric MA-MOX: $(U_{0.74}\ Pu_{0.22}\ Am_z\ Np_w)O_{2-x}$, (x, z, w) = (0.01, 0.02, 0.02) and (0.02, 0.035, 0.005).	Laser heating and analysis of pyrometer thermograms: onset of melting detected by the appearance of vibrations in the signal of a probe laser reflected by the sample surface (RLS technique).
Fouquet-Métivier et al.[39]	Fresh, hypo-/hyper-stoichiometric Am-MOX: Pu content = 28 at.%, Am content = 1 – 2 at.%, O/M = 1.98 - 2.05.	Laser-flash tests on samples in a self-crucible setup: 8 successive shots on same sample, recording of pyrometer thermograms. Combined MD (CALPHAD) modelling to derive corresponding phase diagrams.

value. The variation is hence supposed to be negligibly small also in the operating temperature range of fast reactor MOX fuels [22]. In addition to the experimental works, Table 1 includes two publications on MD-calculated thermal conductivity of MA-MOX fuels [27,28]. Both refer to stoichiometric, fully dense Am-MOX with 30 at.% Pu content, but cover wide ranges in terms of temperature (up to melting temperatures, although melting is not accounted for by MD simulations) and Am content (up to 25 at.%, hence well beyond the limit for the homogeneous recycling of MAs, typically set at 5 wt.%). In both works, the calculated thermal conductivity does not account for neither high temperature effects (electronic contribution), nor the effects of self-irradiation [10], hence it continuously decreases with increasing temperature according to the phononic contribution, showing values at low temperatures higher than the experimental ones. The effect of the Am inclusion into the material lattice is smooth, especially at higher temperatures, while noticeable at 500 K according to [28]. The uncertainties in the MD calculations, associated to the thermal conductivity values reported by [27], consist in around 20% of the values at room temperature, while the uncertainty sensibly decreases with increasing temperature.

As for the MA-MOX melting temperature, the available literature works (Table 2) agree on the decreasing effect (although slight) of increasing MA contents [23,31,32] and of increasing fuel burn-up [31,33,34]. Furthermore, among the references of Table 2 only Kato et al., 2008 [32] shows the impact of a varying fuel plutonium content, but the decrease of melting temperature with increasing Pu is confirmed by the majority of experimental (e.g., [35–37]) and Molecular Dynamics [15,38] studies on MOX fuels (at least in the current ranges of interest for fast reactor and Gen-IV applications, i.e., Pu content < 50 wt.% and $1.90 < O/M < 2.00$).

Instead, the state-of-the-art literature does not show uniform agreement on the dependence of the MOX and MA-MOX melting (solidus) temperature on the deviation from fuel stoichiometry (with respect to $O/M = 2.00$). According to most authors the melting temperature should decrease with increasing deviation from stoichiometry (in the hypo-stoichiometric range and supposedly also in the hyper-stoichiometric one [19,32,33,35]), but a few of recent works, both experimental (e.g., Kato et al. [22]) and MD [38,39], indicate the opposite. In particular, these MD (CALPHAD) calculations [38,39] show a maximum melting temperature around $O/M = 1.98$ and not 2.00, as commonly accepted from the experimental point of view. Nevertheless, these considerations must take into account the reported, significant uncertainty on the fuel O/M ratio upon measurement, due to the oxidation of the samples during the successive laser shots of the experimental procedure [39]. The experimental uncertainty on the melting temperature is also indicated, being consistent with the state-of-the-art one from literature, i.e., around 2% ($\sim$ 60 K) of the measured values [23,32,35,39]. Quantitative indications about the impact of Am and Np additions (1.6 at.% each) in MOX fuels are reported by [22], causing a decrease of the MOX melting temperature of 2–4 K (at deviations from stoichiometry of $\sim$ 0.02 and 0.04, respectively, Table 2). Instead, the burn-up degradation effect is quantified by Konno et al. [31], showing that the extent of decrease of the MA-MOX melting temperature is 5, 4 and 3 K per 10 GWd/t at 50, 100 and 150 GWd/t, respectively [31], a trend qualitatively confirmed by the same authors in their later work [33]. Among the references for the MA-MOX melting temperature (Table 2), Morimoto et al. [40] and Tanaka et al. [34] consider the presence of simulated fission products in the lattice of sintered MA-MOX pellets (although the representativeness of data from SIMFUELS is still to be assessed). In particular, Morimoto et al. focus on the dependence of the melting temperature of (30 at.% Pu, 2 at.% Am, 2 at.% Np) on the deviation from stoichiometry, indicating an unexpected decrease of the melting temperature towards fuel stoichiometry as well [40]. Instead, Tanaka et al. analyse the burn-up dependence in Am-MOX, since the considered compositions are representative of fresh fuel and of high burn-up conditions (150 and 250 GWd/t_{HM}, HM: heavy metal) [34]. The measured melting temperature values are consistent with the expected burn-up degradation, i.e., lower (accounting for the significant uncertainties) than the values measured on fresh fuel or on samples at lower burn-up.

In Tables 1 and 2, the aforementioned literature works accessible to the authors and providing experimental measurements or MD calculations of MA-MOX thermal conductivity and melting temperature are listed. The available state-of-the-art data concern hypo-stoichiometric and (mainly) stoichiometric MA-MOX fuel. The description of the kind of measured/simulated fuel and of the measurement/calculation technique employed is included.

State-of-the-art correlations

The experimental data on MA-MOX thermal conductivity, collected in Table 1, have been in most cases exploited by the same authors as a basis (fitting datasets) to propose correlations representative of those specific data. The developed correlations for the MA-MOX thermal conductivity, currently available in literature, are summarized in Table 3. They generally include only the lattice vibration (phononic) contribution, expressing the temperature dependence in the form $(A+BT)^{-1}$ and describing well the data measured at temperatures < 1800 K [24–26]. In these works, the A and B coefficients of the phononic contribution to thermal conductivity are corrected to include additional MA-related dependencies. Specifically, the inclusion in correlations of the Am effect for stoichiometric Am-MOX is performed by [24], the sole effect of the deviation from stoichiometry of (30 at.% Pu, 2 at.% Am) Am-MOX is represented by [25], while both the Am and Np content effects in MA-MOX are considered by [26]. Also, Prieur et al. [23] model the thermal conductivity of MA-MOX (with up to 3.5 at.% Am and 2 at.% Np contents) with only the phononic contribution, for temperatures up to 1600 K. These past works on MA-MOX all agree in proposing a higher impact on the thermal conductivity (i.e., stronger degradation) due to minor actinides in Am-MOX fuels than in Np-MOX, although the effect is anyway small in percentage with respect to a reference U-Pu MOX thermal conductivity. The degradation of the thermal conductivity of mixed-oxide fuels, already analysed in detail in [19], is supported by theoretical considerations, some of which are also included in [24–26], and experimentally observed in various types of materials and nuclear fuels [47–49]. Moreover, the MA impact proves to be well represented in the A coefficient, while B can be considered independent of the MA content (at least for small minor actinide contents < 5 at.%, but confirmed also for 10 at.% Am content by [46]).

Kato et al., [22] extends the usual modelling at low temperatures, therein based on [25,26], to high temperatures, introducing in the proposed thermal conductivity correlation for MA-MOX an additional electronic contribution exponential in the temperature, based on data from [50] (not accessible to the authors). This kind of electronic contribution to thermal conductivity can be found also in correlations describing UO_2 and U-Pu MOX fuels for application in both thermal and fast reactors [16,19,51,52]. Although Kato et al., reports a couple of measurements of irradiated MA-MOX fuels (beginning-of-life conditions), they are not sufficient to represent a burn-up effect in that correlation, which is then recommended only for fresh MA-MOX [22]. Table 3 highlights that none of the state-of-the-art correlations include the evolution of MA-MOX thermal conductivity with fuel burn-up, which is mainly due to the scarcity of current experimental data linked to the difficulties in handling Am-bearing materials during the fabrication process and post-irradiation examinations. As a consequence,

Table 3
List of state-of-the-art thermal conductivity correlations, available in the open literature or employed by FPCs, for MA-MOX fuel. The dependencies included by each correlation are indicated with X, while for the missing dependencies the corresponding values of the fitted data (for which the correlation is in principle valid) are reported.

Correlation	Temperature	O/M	Pu content	Am content	Np content	Porosity	Burn-up
Morimoto et al. [24]	X	2.00	30 at.%	X	0	X	0
Morimoto et al. [25]	X	X	30 at.%	2.2 at.%	0	X	0
Morimoto et al. [26]	X	2.00	30 at.%	X	X	X	0
Kato et al. [22]	X	X	30 at.%	X	X	X	0
Prieur et al. [23]	X	1.99 / 1.98	22 at.%	2 / 3.5 at.%	2 / 0.5 at.%	94.8 / 94.6% TD	0
TRANSURANUS, SUPERFACT-1 [16]	X	2.00	0	25 / 0 at.%	25 / 50 at.%	95.5 / 95% TD	0

Table 4
List of state-of-the-art melting temperature correlations, available in the open literature or employed by FPCs, for MA-MOX fuel. The dependencies included by each correlation are indicated with X, while for the missing dependencies the corresponding values of the fitted data (for which the correlation is in principle valid) are reported.

Correlation	O/M	Pu content	Am content	Np content	Burn-up
Konno et al.[31]	1.95 - 1.98	X	X	0	X
Konno et al.[33]	X	X	X	0	X

neither the impact of fission products (dissolved or precipitated), nor radiation-induced lattice defects or produced by sample self-irradiation (α-decay) is at present accounted for as in e.g., the model developed by Sobolev et al. [10]. Potential developments in this direction could also follow the approach proposed by Ikusawa et al. for MOX fuels [53]. Nevertheless, the correlation by Kato et al., [22] is employed in a recent work to evaluate the thermal performance of Am-MOX fuel pins irradiated up to very low burn-up (beginning-of-life conditions) in the Joyo reactor [54], or also in the DIRAD-TRANSIT code system developed at the Japan Atomic Energy Agency for simulating the thermal behaviour of MA-MOX fuels under irradiation [55]. None of the existing correlations for the MA-MOX thermal conductivity (Table 3) is comprehensive and inclusive of the Pu content effect combined with the MA one.

State-of-the-art fuel performance codes are typically equipped with thermal conductivity correlations for U-Pu MOX fuels, applied also to MA-MOX. The effect of the minor actinide addition on the degradation of the thermal conductivity property is not specifically represented since currently assessed as small in both fresh/irradiated conditions, and therefore neglected. The TRANSURANUS FPC [16] includes two thermal conductivity correlations, based on specific data measured at JRC-Karlsruhe on MA-bearing fuels fabricated for irradiation during the SUPERFACT-1 campaigns [3]. The considered fuels are (U, Am, Np)O_2 with 25 at.% Am, 25 at.% Np contents and (U, Np)O_2 with 50 at.% Np content, hence representative of the heterogeneous fuel strategy. The models developed and implemented in the code target only the temperature dependence of thermal conductivity, but are independent of the fuel O/M, Pu content and burn-up.

As the MA-MOX thermal conductivity correlations, also the existing melting temperature correlations have been derived separately by different authors, relying on their own set of measurements without integrating with available data from previous works. Table 4 summarizes the state-of-the-art correlations for the melting temperature of mixed-oxides accounting for the effect of minor actinides. Only two correlations from the same authors are available in the open literature, but actually the most recent one [33] can be considered as the update and extension of the previous one [31] including the dependence on the deviation from fuel stoichiometry.

Konno et al. [31] proposes a correlation which is simpler in form, obtained by fitting experimental data measured on fuel samples irradiated up to 124 GWd/t_{HM} in the Japanese experimental fast reactor Joyo. Samples were then canned in tungsten capsules for melting tests. The correlation was derived by applying a combined multi-variable and experimental regression analysis, assuming additivity of the different dependencies within the dataset ranges and modelling the effect of actinides (Pu and Am) according to the ideal solution model. The analyses led to a first order dependence on the Pu and Am contents, while a quadratic dependence on the fuel burn-up was proposed. Instead, the correlation by Konno et al.[33] includes all the main dependencies of interest, i.e., fuel burn-up, stoichiometry, plutonium and americium contents[1], based on a set of data (still from irradiation campaigns in the Joyo reactor) representative of the deviation from stoichiometry effect (in the hypo-stoichiometric range). The resulting correlation features a quadratic dependence on the Pu content, besides the quadratic one on fuel burn-up and mixed-effect terms involving the Am content. Both models are applicable to a wide range of burn-up values, i.e., up to 124 and 110 GWd/t_{HM}, respectively. Instead, as indicated by Table 4, the neptunium content effect is currently not represented, and also, the considered data were deemed not suitable to include in the correlations an explicit dependence of the MA-MOX melting temperature on the soluble fission products, which are actually recognized to sensibly impact the fuel melting temperature [31].

Based on the available experimental data collected in Tables 1 and 2, novel correlations for the thermal conductivity and melting temperature of minor actinide-bearing MOX fuel are herein derived, extending correlations for U-Pu MOX previously published by the same authors [19,30], and compared to the literature correlations collected in Tables 3 and 4 in terms of accuracy in predicting the state-of-the-art measurements. As a modelling choice, both correlations are obtained from a best fit of the experimental data, while the data provided by molecular dynamics calculations are kept for comparison and additional assessment. This is justified by the discrepancies and novelties brought about by the MD calculations with respect to the state-of-the-art experimental knowledge on both properties as mentioned in Section 2, e.g., higher thermal conductivity values at low temperatures, or a maximum melting temperature at hypo-stoichiometric fuel rather than for stoichiometric fuel. Possibly, MD simulation results could be exploited as part of the fitting dataset in future developments, to refine the modelling of thermal properties and further extend

[1] The effect of actinides is included in the correlation by Konno et al., 2002 [33], based again on the ideal solution model. The applied method still consists in an experimental regression analysis under the hypothesis of additive effects.

the range of validity of the herein presented correlations, covering values of the correlation variables at which the experimental information is currently missing or poor (e.g., high temperatures > 2000 K, high Pu contents > 50 wt.%, high MA content > 10 wt.%). A similar approach has been recently adopted for the modelling of heat capacity of MOX fuels [56].

Novel correlation for thermal conductivity of MA-MOX fuels

As fitting dataset for the modelling of thermal conductivity of MA-MOX fuels, all the experimental works listed in Table 1 have been considered, in light of the limited amount of information available in the open literature. Most of the currently available works provide measurements on fresh MA-MOX fuels, i.e., Morimoto et al. works [24]–[26] on stoichiometric Am-MOX, hypo-stoichiometric Am-MOX and stoichiometric Np-MOX, respectively; Prieur et al. data on both Am and Np-bearing hypo-stoichiometric MOX [23]; the recent Yokohama et al. data on stoichiometric MOX with higher Am content (10 at.%) [46]. Only one work is currently available in the open literature about irradiated MA-MOX, by Kato et al., [22], providing two data points corresponding to a low MA content (1.6 at.% of both Am and Np), besides the single, low temperature of measurement (1273 K) and the very low fuel burn-up (< 1% FIMA, Fissions per Initial Metal Atom), from short irradiation campaigns performed in the Japanese fast reactor Joyo (Table 1). In general, the available measurements correspond to a temperature range from about 300 K up to 1800 K, deviation from fuel stoichiometry up to 0.085 (in the hypo-stoichiometric range), 30 at.% Pu content (apart from Prieur's measurements, at 22 at.% Pu content [23]), Am content up to 10 at.%, Np content up to 12 at.%, porosity up to ∼ 16% Theoretical Density (although most of the data are normalized to 100% TD), fresh fuel or at very low burn-up [22] (consistent with reactor start-up situations).

As for the recently proposed, novel thermal conductivity correlation for U-Pu MOX fuels [19], also the model development for MA-MOX is performed in two steps. First, a correlation for fresh MA-MOX thermal conductivity (k_0) is derived, fitting the regressors associated to minor actinides on the experimental data of fresh MA-MOX. Then, a correlation describing the thermal conductivity evolution during fuel irradiation is obtained by including k_0 in a burn-up dependant formulation (k, [19]), fitted on the available data measured on both MOX and MA-MOX irradiated fuels (hence, keeping the validity of the correlation for U-Pu MOX).

The adopted modelling choice, justified by the reported small effect of minor actinide inclusions on the MOX thermal conductivity [22] and by the limited amount of available experimental data, consists in applying the same methodology and the same formulation proposed for the MOX thermal conductivity [19,30]. It is a physically grounded expression k_0(T, x, [Pu], p) including two temperature-dependent contributions (lattice vibration (phononic) and electronic, dominant at low and high temperature, respectively), corrected with the inclusion of plutonium and deviation from stoichiometry-dependent terms in the lattice contribution, and of a porosity factor. This comprehensive correlation is herein extended to account for specific dependencies on the contents of the minor actinides Am and Np, under the assumption that the same coefficient values of the MOX correlation [19,30] hold also for the MA-MOX thermal conductivity[2]. The additional dependencies on the Am and Np contents are introduced modifying the A and B terms of the lattice vibration contribution, similarly to the Pu content effect (and the deviation from stoichiometry one). Hence, the comprehensive functional form of the thermal conductivity correlation for fresh MA-MOX is:

$$k_0(T, x, [Pu], [Am], [Np], p) = \left(\frac{1}{A + BT} + \frac{D}{T^2} e^{-\frac{E}{T}}\right)(1 - p)^{2.5} \quad (1)$$

with $A = A_0 + A_x \cdot x + A_{Pu}[Pu] + A_{Am}[Am] + A_{Np}[Np]$ and $B = B_0 + B_{Pu}[Pu] + B_{Am}[Am] + B_{Np}[Np]$, i.e., with the Am and Np content effects supposedly introduced both in the A and B terms, in absence of precise indications available in literature about an assessed formulation [22,23,26]. The variable T is for the temperature (K), x is the deviation from fuel stoichiometry, p is the porosity (/ TD), while [Pu], [Am], [Np] are the plutonium, americium and neptunium (local) concentrations, respectively. The reader is referred to [19,30] for the meaning of and further details about the other terms of Eq. 1. In addition to the coefficients already fitted on the MOX fuel data (i.e., A_0, A_x, A_{Pu}, B_0, B_{Pu}, D, E, [19, 30]), A_{Am}, A_{Np}, B_{Am} and B_{Np} are the additional correlation coefficients for the minor actinide effects, to be fitted on the set of fresh MA-MOX experimental data. The validity of the thermal conductivity contribution from the classical phonon transport model (i.e., the lattice vibration term $(A + B \bullet T)^{-1}$) has been confirmed also for MA-MOX at low temperatures by [23], up to about 1400 K.

Following the same assessment approach adopted for the fresh MOX correlation [19,30], the significance of the minor actinide-related contributions to the correlation (depending on the chosen fitting dataset) is evaluated relying on a statistical analysis. A multi-dimensional fit has been performed using both MATLAB tools [57] and the R code [58], an open source software with built-in statistical analysis capabilities, to obtain the regressor values, the related p-values, the confidence intervals and the fit residuals. The significance of each MA-related regressor of the supposed functional form is assessed considering the associated p-value as figure of merit, compared to a threshold p-value of 5% (corresponding to a 95% confidence on the significance of a regressor). Hence, a regressor is kept in the assessed correlation if the associated p-value is below 5%, otherwise it is rejected as statistically insignificant, i.e., not well represented by the fitting dataset. It is worth highlighting that the p-values and all the results of the fitting procedure depend on the dataset on which the fit is performed [19,30]. The coefficient initial values, required by the non-linear fit iterations searching for convergence, were set equal to the corresponding values employed by existing correlations [22,24,26]. Moreover, the stability of the fit results and their independence on the initial values was tested and verified, within reasonable ranges of the initial values themselves.

As for the statistical assessment of the correlation, it was tested against the entire set of available experimental data (Table 1) as well as against sub-sets of data corresponding to a dependence on the sole Am or Np content. The aim of these partial fits is to achieve higher confidence on the significance of each correlation regressor, focusing only on the p-values. The resulting p-values allow the inclusion in the correlation of the supposed four MA-related regressors (i.e., A_{Am}, A_{Np}, B_{Am}, B_{Np}), with the best p-value associated to A_{Am} (< 1%, while the others are closer to the 5% threshold but still lower than 5%). The fit of the statistically assessed formulation of Eq. 1 on the set of fresh MA-MOX experimental data (Table 1) leads to the results collected in Table 5, in terms of coefficient values, calculated standard errors and associated p-values. The final regressor values were obtained by imposing their positivity as a constraint, in order to guarantee their physical sense, i.e., the degradation of the MA-MOX thermal conductivity with increasing Am and Np contents, as expected from experimental observations (Table 1) and from theoretical considerations about phonon interactions with lattice defects [26,59,60]. The regressor values reported in Table 5 hold for americium and neptunium concentrations ([Am], [Np]) expressed in atomic frac-

[2] This assumption relies on the current predominance of the data available on MOX fuels [52,61–65] with respect to MA-MOX ones [23–26,46].

Table 5
Results of the fit of the statistically assessed k_0(T, x, [Pu], [Am], [Np], p) correlation (Eq. 1) on the set of available experimental data on fresh MA-MOX thermal conductivity [23–26,46] for what concerns the MA-related regressors. The other coefficients of Eq. 1 are assumed equal to the values holding for U-Pu MOX fuel [19,30].

Regressor	Units	Estimate	Std. Error	p-values
A_{Am}	m K W^{-1}	0.596	0.377	$8.45 \bullet 10^{-3}$
A_{Np}	m K W^{-1}	$2.22\ 10^{-14}$	-	$4.02 \bullet 10^{-2}$
B_{Am}	m W^{-1}	$5.47\ 10^{-4}$	$4.16\ 10^{-4}$	$4.76 \bullet 10^{-2}$
B_{Np}	m W^{-1}	$2.48\ 10^{-14}$	-	$3.69 \bullet 10^{-2}$

tion; the thermal conductivity k_0 (Eq. 1) is calculated in W m^{-1} K^{-1}.

From Table 5, it is worth highlighting the main effect of the Am content on the fresh MA-MOX thermal conductivity, while the Np content effect proves negligible. In particular, the value of coefficient A_{Am} is dominant (among the minor actinide-related effects) and in line with the corresponding value obtained by previous literature works [22,24,26]. This can be explained considering the α-activity of Am-241, which sensibly contributes in producing more lattice defects in the fuel material, hence determining a lower thermal conductivity of Am-MOX samples compared to U-Pu MOX or Np-MOX ones [23]. Furthermore, differences in the local fuel stoichiometry/oxygen potential determined by the presence of Am or Np, reported by [23], may contribute to different (local) thermal conductivity values. This is mainly due to the presence of trivalent Am, giving rise to vacancies in the Am-MOX material and inducing a reduction of the thermal conductivity of Am-MOX. Instead, little experimental information is available about Np-bearing MOX and only from samples with low Np content [23,26], hence the herein derived effect of the Np concentration, which could be further investigated and better assessed when additional data will become available. The obtained values of the A_{Am} and B_{Am} coefficients provide effects on the lattice vibration contribution to thermal conductivity, $(A + B \bullet T)^{-1}$ (i.e., $A_{Am} \bullet [Am]$ and $B_{Am} \bullet [Am] \bullet T$), which are compatible with the orders of magnitude of A and B [19,30]. Moreover, the dependency on the Am content is stronger in A than in B, in line with previous experimental findings showing a B value which can be assumed as constant or independent of the MA content [22,24–26], and in line with theoretical considerations since the A term represents the interaction of phonons with lattice imperfections (e.g., defects, impurities).

To account for the burn-up effect on the MA-MOX thermal conductivity, the modelling choice is coherent with the formulation already proposed for U-Pu MOX fuels [19,30], consisting in an exponential, asymptotic degradation of the thermal conductivity with fuel burn-up (Eq. 2). This is suggested first of all by physical grounds, i.e., the accumulation with increasing fuel burn-up of fission products and point defects in the material lattice, up to saturation. This increases the phonon scattering effect lowering the thermal conductivity, and the saturation value is represented by an asymptotic thermal conductivity accounting for thermal recovery processes, as explained in [19,30]. Moreover, the limited effect of minor actinide inclusions in MOX fuels, equivalent in kind to the Pu content one, and the scarce amount of data currently available on irradiated MA-MOX [22] support the choice of relying on the same burn-up formulation for the irradiated MA-MOX thermal conductivity. Hence, the proposed correlation for MA-MOX fuels, inclusive of the burn-up effect, reads:

$$k(T, x, [Pu], [Am], [Np], p, bu) = k_{inf} + (k_0 - k_{inf}) \cdot e^{-\frac{bu}{\varphi}} \quad (2)$$

where $k_0 = k_0(T, x, [Pu], [Am], [Np], p)$ is the thermal conductivity of fresh MA-MOX calculated using Eq. 1 (employing the coefficient values collected in Table 5), bu is the fuel burn-up in GWd/t_{HM},

Table 6
Results of the best fit of the k(T, x, [Pu], [Am], [Np], p, bu) correlation (Eq. 2) on the set of available experimental data on the thermal conductivity of irradiated MOX and MA-MOX [22,61,62].

Regressor	Units	Estimate	Std. Error
k_{inf}	W m^{-1} K^{-1}	1.755	-
φ	GWd/t_{HM}	128.75	8.59

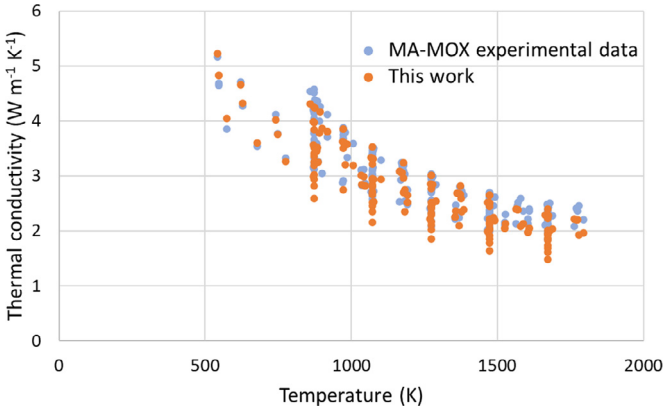

Fig. 1. Temperature dependence of the MA-MOX thermal conductivity experimental data (light blue dots, Table 1), compared to the corresponding predictions provided by the novel correlation developed in this work (orange dots, Eqs. 1 and 2 with coefficients in Tables 5 and 6) (For interpretation of the references to color in this figure legend, the reader is referred to the web version of this article).

k_{inf} is the asymptotic thermal conductivity at high fuel burn-up and φ is a correlation coefficient to be fitted on the irradiated fuel data. As fitting dataset for the burn-up effect, the accessible experimental data about both fast reactor MOX [19,30] and MA-MOX fuels have been considered, to overcome the limitation of too few information currently available about irradiated MA-MOX. Hence, the open literature data by Yamamoto et al. on MOX at low and moderate burn-up ([61], open literature) and the measurements of NESTOR-3 fast reactor MOX fuel at high burn-up performed during the ESNII+ European Project [62], already considered in [19,30], are herein complemented by the only two available data points concerning irradiated MA-MOX (at very low burn-up, [22]). Consequently, the considerations leading to the best value for k_{inf}, based on MOX fuel experimental information [19,30], are deemed still valid for MA-MOX. Indeed, the values of thermal conductivity reported by [22] are compatible with MOX fuel data. Based on this value of k_{inf}, the best fit of Eq. 2 on the considered dataset leads to the same value for the coefficient φ, which is reasonable considering the current predominance of the MOX data over the MA-MOX ones. The formulation of Eq. 2 is hence still applicable to MOX fuel, setting zero Am and Np contents, and applicable to fresh fuel, since at zero burn-up $k(T, x, [Pu], [Am], [Np], p, bu = 0) = k_0(T, x, [Pu], [Am], [Np], p)$, from Eq. 2. The burn-up-related coefficients are collected in Table 6.

The comparison between the correlation predictions (Eq. 1 and 2 with coefficients in Tables 5 and 6) and the available MA-MOX experimental data (Table 1), considered as fitting dataset, is shown in Figs. 1 and 2, in terms of temperature dependence and validation plot, respectively. The agreement between data and predictions is remarkable, both at low and high temperatures, with slight over-estimations at low temperatures (< 700 K) and slight under-estimations at higher temperatures, where more data are available. The satisfactory accuracy is particularly indicated by Fig. 2, including the side-diagonals corresponding to the typical experimental uncertainties on MOX thermal conductivity reported in literature,

Table 7
Root mean square error of the correlation for the MA-MOX thermal conductivity developed in this work, compared to the state-of-the-art literature correlations for MA-MOX fuel accounting for the MA effect, over the set of data of fresh and irradiated MA-MOX [22–26,46].

	Morimoto et al.[24]	Morimoto et al.[26]	Kato et al.[22]	This work
Root mean square error (rmse)	0.08	0.12	0.07	0.10

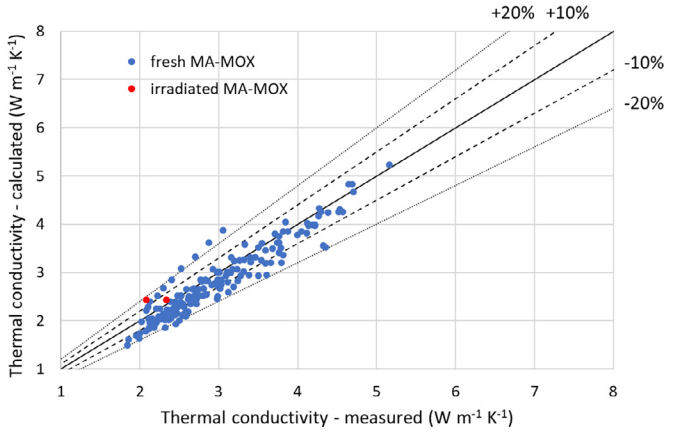

Fig. 2. Comparison between the experimental data of both fresh and irradiated MA-MOX thermal conductivity (Table 1) and the corresponding predictions provided by the novel correlation developed in this work (Eqs. 1 and 2 with coefficients in Tables 5 and 6).

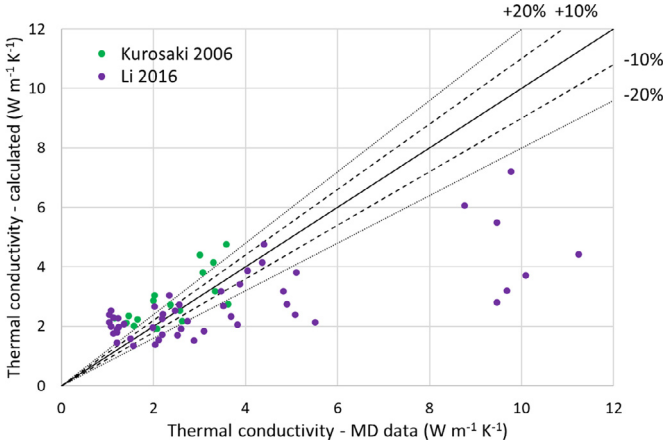

Fig. 3. Comparison between the molecular dynamics data of MA-MOX fuel thermal conductivity ([27,28], Table 1) and the corresponding predictions provided by the correlation developed in this work (Eqs. 1 and 2 with coefficients in Tables 5 and 6). The uncertainties associated to the data reported by Kurosaki et al. ([27], green dots) consist in up to 22% of the MD-calculated values (For interpretation of the references to color in this figure legend, the reader is referred to the web version of this article).

i.e., between 10 and 20% of the measured values [52,61–65] (while no specific uncertainty indications on the measured MA-MOX thermal conductivities are reported by the authors [22–26,46]). The only series of points outside the 20% deviation band in Fig. 2 correspond to data measured on samples with high deviation from stoichiometry [25] (i.e., $x > 0.05$, which is the limit of the applicability range of the proposed correlation), where defect clustering may occur [66]. The novel correlation proves suitable to predict the thermal conductivity of low burn-up MA-MOX fuel according to the only accessible literature reference ([22], red points in Fig. 2).

The ranges of applicability of the herein proposed correlation for the thermal conductivity of MA-MOX, obtained by extending a previously developed correlation for MOX fuels [19,30], mainly correspond to the ranges covered by the available experimental data:

- Temperature, T: [500, 2700] K
- Deviation from stoichiometry, x: extended to [0, 0.05] (hypo-stoichiometric range)
- Plutonium content, [Pu]: [0, 45] at.%
- Americium content, [Am]: [0, 10] at.%
- Neptunium content, [Np]: [0, 12] at.%
- Porosity, p: extended to [0, 10]% TD
- Burn-up, bu: [0, 130] GWd/t_{HM}.

The applicability of the correlation to high temperatures, high plutonium contents and high fuel burn-up levels is guaranteed by the available experimental data on MOX fuels [19,30], while the predictions at high deviations from fuel stoichiometry (above 0.05) and high porosities (above 10% TD) are not deemed reliable, due to deviations from the measured thermal conductivity values higher than the upper experimental uncertainty, i.e., 20% of the measured data. As already proposed in [19], data assimilation techniques [67] could be envisaged for a progressive upgrade of the correlation and further extension of its ranges of applicability, as soon as more and representative experimental results on MOX and MA-MOX fuels for fast reactor and transmutation applications will become available.

Table 7 reports the root mean square error (rmse) of the novel correlation on the entire set of experimental data of MA-MOX thermal conductivity, including both fresh and irradiated MA-MOX (Table 1), compared to the rmse of three literature correlations developed for specific MA-MOX datasets and herein considered for comparison [22,24,26]. The average error associated to the novel correlation proves small, improves that from [26] and is comparable with the rmse obtained with the correlations from [22,24], hence the comprehensive correlation herein developed can be considered satisfactory.

The novel correlation for the MA-MOX thermal conductivity is also assessed against the results of the only two sets of values from molecular dynamics simulations available in the open literature ([27,28], Table 1). The results of this assessment are shown in Fig. 3, including the deviation bands corresponding to the typical experimental uncertainties reported in literature (i.e., between 10 and 20% of the measured data) [19,30]. The cloud of points is reasonably close to the perfect agreement between predictions and data at low thermal conductivity values (1 – 4.5 W m^{-1} K^{-1}), especially considering the uncertainties currently involved in the MD calculations, i.e., up to 22% as reported by [27]. The significant deviations from the high thermal conductivity values calculated by means of molecular dynamics correspond to low temperatures (data at 500 K [28], lower limit of applicability of the novel correlation) or to high Am contents between 15 and 25 at.% [28], which are outside the range of validity of the correlation, and show that the correlation is conservative. It should be kept in mind that the MD simulations do not consider at present the effects of self-irradiation related to α-decay [10], which is instead accounted for by the experimental measurements and therefore also in the fitted correlation herein proposed.

Novel correlation for melting temperature of MA-MOX fuel

Among the available state-of-the-art experimental measurements of MA-MOX melting temperature, collected in Table 2, the ones selected as fitting dataset for the novel melting temperature correlation for MA-MOX fuel cover both fresh and irradiated material, although the number of data points currently available is lower compared to MA-MOX thermal conductivity. About fresh MA-MOX, literature works by Kato et al., [32], Prieur et al. [23] and the recent measurements performed at JRC-Karlsruhe by Fouquet-Métivier et al. [39] have been considered. Among Kato et al. measurements [32], only those performed in rhenium inner capsules (sealed into outer tungsten capsules) have been selected, due to the confirmed strong contamination by W of the molten fuel material, which heavily affects the measured melting temperature [35,68]. Kato et al. data [32] all correspond to stoichiometric MA-MOX, bearing both Am and Np. Data on hypo-stoichiometric fuels are instead provided by Prieur et al. (Am, Np-MOX) and Fouquet-Métivier et al. (Am-MOX). The latter includes also measurements on hyper-stoichiometric samples, which are beyond the scope of the present analysis, focused on the hypo-stoichiometric range (applied for mixed-oxide fuels fabricated for fast reactor applications). The MA-MOX data by Morimoto et al. [40] include the simulated effect of fission products, but have been excluded from the analysis due to a reported behaviour of the melting temperature as a function of the deviation from stoichiometry (i.e., decreasing with decreasing off-stoichiometry), which deviates from the majority of experimental and modelling works in the literature for various types of oxide fuels [16,19,33,69]. Hence, the suitable data about irradiated MA-MOX are those provided by Konno et al., [33], already considered in [19,30] and corresponding to fuel irradiated up to high burn-up ($\sim$ 110 GWd/t_{HM}), and by Kato et al., [22], on very low burn-up fuel samples ($<$ 1% FIMA). Previous data on irradiated MA-MOX by Konno et al. [31] are not used here because the measurements were performed in W capsules, leading to sensibly lower measured melting points. The single data point at very high burn-up (150 GWd/t_{HM}) available from Tanaka et al. [34] is kept for additional comparison and considerations, since it includes also the effect of simulated fission products. In summary, the selected datasets of both fresh and irradiated MA-MOX fuels (from Table 2) correspond to low MA contents (up to 3.5 at.% Am content and 2 at.% Np content, with the majority of data concerning Am-MOX) and to Pu contents that are in line with values of interest for fast reactor and Gen-IV applications (between 16 at.% and 60 at.% Pu).

The correlation herein proposed for the melting (solidus) temperature of MA-MOX fuel relies on the same modelling strategy and hypotheses adopted for the already published correlation for U-Pu MOX fuels [19,30]. In a similar way to the modelling of thermal conductivity, the strategy consists in a two-steps model development, foreseeing first a correlation suitable for fresh MA-MOX ($T_{m,0}$), derived by fitting the selected experimental data of fresh MA-MOX. Then, a correlation describing the melting temperature evolution with fuel burn-up is obtained by including $T_{m,0}$ in a formulation fitted on the data measured on irradiated fuel. As in [19], it is assumed that each effect is independent (i.e., additive) and a linearly decreasing dependency of the melting temperature is applied for each parameter as a first approximation, in light of the limited set of available experimental data. Hence, the correlation for fresh U-Pu MOX [19,30] is extended with the inclusion of the Am and Np effects (supposedly acting as the Pu content), reading:

$$T_{m,0}(x,[Pu],[Am],[Np]) = T_{m,UO_2} - \gamma_x\, x - \gamma_{Pu}\,[Pu] - \gamma_{Am}\,[Am] - \gamma_{Np}\,[Np] \quad (3)$$

where (as in [19]) T_{m,UO_2} is the melting temperature of fresh stoichiometric UO_2, i.e., 3147 K according to the recent experimental measurements by Manara et al. [70] recommended by the ESNII+ Catalogue on MOX properties [71]; x is the deviation from fuel stoichiometry, while [Pu], [Am], [Np] are the plutonium, americium and neptunium contents, respectively. The coefficients γ_x and γ_{Pu} were already represented in the correlation for U-Pu MOX fuels [19,30], while γ_{Am} and γ_{Np} are the novel regressors associated to the minor actinide effects, to be fitted on the fresh MA-MOX melting temperature data.

The statistical analysis based on the regressor p-values was performed again applying the R code and MATLAB tools [57,58] and still assuming a threshold p-value of 5%. It reveals the significance of the Am effect but leads to the exclusion of the Np effect, according to the fitting dataset herein considered. Indeed, the p-value associated to the Np-dependent term is sensibly $>$ 5% (48.6%), also testing it as a single effect on the (few) data showing the sole Np-dependence. The amount of available data on Np-bearing fuels is indeed very limited (four data points in total), hence the Np effect on the mixed-oxide melting temperature cannot be properly represented and justified. Moreover, the negligible Np effect on the melting temperature of mixed-oxides suggests that material self-irradiation due to α-decay, among the MA-related effects, mostly drives the decrease of the fresh MOX thermal properties (also of the thermal conductivity, comparing the values of the Am- and Np-related correlation coefficients, Table 5). Indeed, americium is highly α-active, inducing a substantial amount of defects in the fuel microstructure which degrade the nuclear fuel thermal properties.

As a result, the statistically assessed formulation of the correlation for the melting temperature of fresh MA-MOX is established as follows:

$$T_{m,0}(x,[Pu],[Am]) = T_{m,UO_2} - \gamma_x\, x - \gamma_{Pu}\,[Pu] - \gamma_{Am}\,[Am] \quad (4)$$

The best fit of Eq. 4 over the selected set of fresh MA-MOX melting temperature data (from Table 2) yields the results summarized in Table 8, in terms of regressor values, associated standard errors and p-values. In line with the extension of the MOX thermal conductivity correlation to MA-MOX (Section 4), the values of the γ_x and γ_{Pu} coefficients are kept as in the MOX correlation [19,30], while γ_{Am} is obtained by a best fit of the experimental data on fresh MA-MOX fuel. The coefficient values reported in Table 8 hold for T_{m,UO_2} expressed in K and [Pu] and [Am] expressed in at./, and $T_{m,0}$ is calculated in K. The analysis of the trends of the fit residuals, including the Am-dependent term, does not call for the introduction of higher-order terms or mixed dependencies (present instead in the Konno et al., correlation [33]), since all the fit residuals are randomly distributed if plotted against x, [Pu] or [Am].

In the second step of the model development, the expression for the melting temperature of fresh MA-MOX (i.e., $T_{m,0}(x,[Pu],[Am])$ according to Eq. 4, with regressor values in Table 8) is used in a burn-up dependent formulation, still consisting in an exponential, asymptotic decrease of the melting temperature with burn-up, as for the melting temperature of irradiated U-Pu MOX fuels [19,30] and for the thermal conductivity of irradiated MA-MOX fuels (Section 4). This is physically grounded and justified in a similar way as for the thermal conductivity evolution with

Table 8
Results of the best fit of the statistically assessed $T_{m,0}(x,[Pu],[Am])$ correlation (Eq. 4) on the set of selected melting temperature data of fresh MA-MOX [23,32,39]. The values of γ_x and γ_{Pu} are kept equal to those holding for U-Pu MOX fuels [19,30].

Regressor	Units	Estimate	Std. Error	p-values
γ_x	K	1014.15	253.57	$1.21\bullet10^{-2}$
γ_{Pu}	K at./$^{-1}$	364.85	13.96	$< 2\bullet10^{-16}$
γ_{Am}	K at./$^{-1}$	329.5	223.2	$5.65\bullet10^{-4}$

Table 9
Results of the best fit of the $T_m(x, [Pu], [Am], bu)$ correlation (Eq. 5) on the set of selected experimental data of melting temperature of irradiated MA-MOX [22,33].

Regressor	Units	Estimate	Std. Error
$T_{m,inf}$	K	2964.94	34.62
δ	GWd/t_{HM}	41.01	24.25

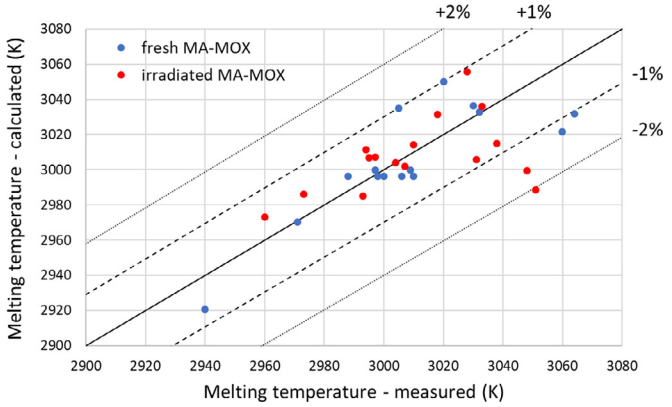

Fig. 4. Comparison between the experimental data of both fresh and irradiated MA-MOX melting temperature (Table 2) and the corresponding predictions given by the novel correlation developed in this work (Eqs. 4 and 5 with coefficients in Tables 8 and 9).

fuel burn-up, i.e., considering the continuous build-up of defects and fission products evolving towards the saturation of the material lattice, confirmed by both experimental observations ([31], showing that the extent of decrease of the MA-MOX melting temperature is 5, 4 and 3 K per 10 GWd/t at 50, 100 and 150 GWd/t, respectively) and results of molecular dynamics calculations (e.g., [15,31]). Hence, the formulation proposed for the MA-MOX melting temperature correlation including the burn-up effect reads:

$$T_m(x, [Pu], [Am], bu) = T_{m,inf} + \left(T_{m,0} - T_{m,inf}\right) \cdot e^{-\frac{bu}{\delta}} \quad (5)$$

where bu is the fuel burn-up in GWd/t_{HM}, $T_{m,0} = T_{m,0}(x, [Pu], [Am])$ is the melting temperature of fresh MA-MOX according to Eq. 4, while $T_{m,inf}$ and δ are the correlation parameters to be fitted on the set of melting temperature data of irradiated MA-MOX. This formulation is consistent with the one previously developed for U-Pu MOX fuel [19,30], setting zero Am and Np contents, and with $T_m(x, [Pu], [Am], bu) = T_{m,0}(x, [Pu], [Am])$ when the fuel burn-up is equal to zero. Fitting Eq. 5 on the irradiated MA-MOX data [22,33] leads to the regressor values reported in Table 9. The values of the coefficients $T_{m,inf}$ and δ only slightly differ from the corresponding values obtained for MOX fuels [19,30], due to the few additional measurements on MA-MOX available in literature (by Kato et al., [22]) besides Konno et al., ones already exploited for the MOX correlation [33].

The comparison between the correlation predictions (Eq. 4 and 5 with coefficients in Tables 8 and 9) and the available MA-MOX experimental data (Table 2) considered as fitting dataset is shown in Fig. 4. The agreement between the predictions and the experimental data is highly remarkable, both concerning fresh and irradiated MA-MOX, since most of the predictions lay within the 1% deviation band from the perfect agreement (i.e., maximum ~ 30 K deviation from the measurements, corresponding to the best experimental uncertainty at the state of the art [32,36,63,72,73]). The entire cloud of points of Fig. 4 is included in the 2% deviation band, hence within the current highest experimental uncertainty (~ 60 K).

Fig. 5 compares the behaviour of the novel correlation for the MA-MOX melting temperature, as a function of burn-up and Am content, with the two state-of-the-art correlations available in the open literature [31,33]. In terms of fuel burn-up, the novel correlation exhibits an exponential, asymptotic decreasing trend, leading to higher melting temperature values predicted at high burn-up (similarly to the novel correlation recently proposed for U-Pu MOX fuels [19,30]). This reflects the characteristics of the fuel microstructure at high burn-up, when the formation of a highly porous High Burn-up Structure (HBS) in the low temperature (peripheral) fuel region determines a reduction of the fission product concentration in the lattice [74–76]]. This process, together with a large fractional release of gaseous fission products occurring in fast reactor mixed-oxide fuels at high temperature, causes a reduced rate of decrease of the fuel melting temperature. The predictions of the correlations at high burn-up are compared with the only experimental measurement available, from [34] at 150 GWd/t_{HM}. The novel correlation proves to be the least accurate in this prediction, but the deviation (~ 50 K) is within the reported experimental uncertainties at the state of the art (30–60 K, as already discussed in [19]). Moreover, it must be considered that this single experimental point accounts for the (degrading) effect of simulated fission products on the melting temperature, which is not explicitly represented by the novel correlation herein developed but included in the burn-up dependence. In terms of the Am content effect, the novel correlation features a slighter dependence, which can be considered more reliable since fitted on a wider set of experimental data [22,23,32,33,39]. Instead, the dependence of the melting temperature on the Am content is much more pronounced in the Konno et al. correlations, fitted only on limited sets of own data subjected to significant uncertainties [31,33]. More experimental data are therefore highly recommended for assessing the dependency on the Am content, which is planned in the framework of the PATRICIA H2020 European Project [11].

The novel melting temperature correlation (Eqs. 4 and 5, with coefficients in Tables 8 and 9) is also assessed against a set of molecular dynamics data available in the open literature (by Galvin et al., on U-Pu MOX [15], hence the americium content in the correlation is set to zero for a proper comparison). These MD-calculated data concern stoichiometric MOX on the entire range of Pu contents from UO_2 to PuO_2, showing a Pu content effect on the melting temperature in line (considering the existing high uncertainties) with experimental measurements corresponding to plutonium contents up to 60 at.% [32,35,36,77], hence including the range of interest for MOX fuel applications in fast reactors and Generation IV concepts [1,2]. The MD-calculated melting points continuously decrease at higher Pu contents above 60 at.%, a region in which strong disagreements among different authors are reported in literature [32,72,77]. The uncertainties associated to the calculated values are around 1% or less, comparable with the current experimental uncertainties (between 30 and 60 K, i.e., 1–2% of the data [19]). The results of this assessment are presented in Fig. 6, showing satisfactory predictions since the cloud of points lays within the 2% deviation band (corresponding to the upper experimental uncertainty reported in literature, i.e., ~ 60 K [23,32,33,35]). The only exception is represented by the melting temperature of stoichiometric UO_2, which is predicted to be equal to 3147 K according to the present correlation (based on [19,70]), while almost 100 K lower as calculated by [15].

The ranges of applicability of the novel correlation for the melting temperature of MA-MOX fuels are consistent with the ranges covered by the fitted experimental data [22,23,32,33,39]:

- Deviation from stoichiometry, x: [0, 0.06] (hypo-stoichiometric range)
- Plutonium content, [Pu]: [0, 50] at.%

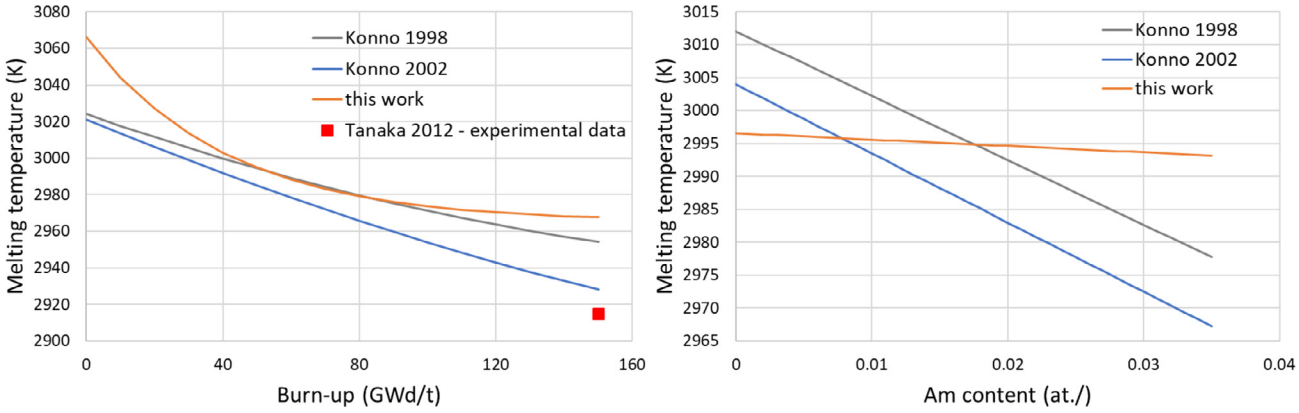

Fig. 5. Behaviour of the novel MA-MOX melting temperature correlation (orange line), as a function of fuel burn-up (left) and Am content (right), compared to the two state-of-the-art correlations for MA-MOX available from the open literature [31,33]. Both plots refer to hypo-stoichiometric MA-MOX with x = 0.002 and Pu content = 20 at.%, while the Am content = 1.8 at.% in the left plot (to reproduce the experimental point from [34]) and the fuel burn-up = 50 GWd/t_{HM} in the right plot.

Table 10
Root mean square error of the novel correlation for the MA-MOX melting temperature developed in this work, compared to the state-of-the-art literature correlations for MA-MOX fuel, over the set of available data on fresh and irradiated MA-MOX [22,23, 32,33,39].

	Konno et al. [31]	Konno et al. [33]	This work
Root mean square error (rmse)	0.017	0.016	0.007

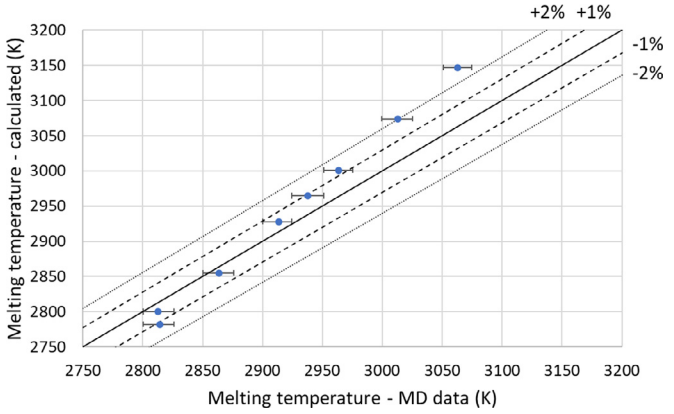

Fig. 6. Comparison between the MD data on MOX fuel melting temperature from Galvin et al. [15] and the corresponding predictions given by the novel correlation developed in this work (Eqs. 4 and 5, with coefficient values in Tables 8 and 9, setting zero Am content). The MD-simulated uncertainties are included as horizontal error bars [15].

- Americium content, [Am]: [0, 3.5] at.%
- Burn-up, bu: extended to [0, 150] GWd/t_{HM}.

Since the MA-MOX correlation herein proposed is an extension of the previously published correlation assessed for U-Pu MOX fuels [19,30] and still includes the application to U-Pu MOX, the range of applicability in terms of deviation from stoichiometry is mainly dictated by the available MOX experimental data [19,30], while the range in plutonium content is limited to 50 at.% due to contradictory results available in literature for the melting temperature of very high Pu content-MOX [15,38,72]. The extension of the range of validity of the novel correlation in terms of fuel burn-up can be justified by the prediction of the experimental point at high burn-up from [34] within the experimental uncertainty, and by the exponential, asymptotic functional form of the correlation.

Table 10 reports the root mean square error of the three correlations (i.e., the novel correlation developed in this work and those by Konno et al. [31,33]) on the entire set of available experimental data, concerning both fresh and irradiated MA-MOX fuels (Table 2). The error of the novel correlation is less than half the errors of the other two literature correlations for MA-MOX [31,33] over the considered data.

Integral application of the novel correlations for MA-MOX fuel

As an illustrative example, the novel correlations for the thermal conductivity and melting temperature of minor actinide-bearing MOX fuels, herein developed (Sections 4 and 5), are employed to simulate the thermal performance of a fast reactor fuel pin. The reference database corresponds to the HEDL P-19 irradiation experiment, performed in the EBR-II reactor (sodium-cooled, open pool type) and consisting in power-to-melt tests of U-Pu MOX fuel (25 at.% Pu content) at beginning-of-irradiation conditions [20]. The experimental data available from the HEDL P-19 irradiation campaign have already been considered for the integral validation of the correlations for the thermal properties of MOX fuels ([19], where the complete details on the HEDL P-19 experiment are collected). In this work, the focus is on a representative pin (# 27) selected from the HEDL P-19 database, showcasing the potential impact of a minor actinide content in the U-Pu MOX fuel. The reference results for the U-Pu MOX are compared to those for an hypothetical Am-MOX fuel with 5 at.% Am content subjected to the same irradiation conditions (i.e., fast power ramps up to fuel melting in beginning-of-life conditions). The Am content here considered corresponds to the upper limit for homogeneous MA-MOX (avoiding cluster effects on the fuel microstructure and properties occurring in heterogeneous fuels [4,5]), and thus maximizes the effect of Am in the mixed-oxide fuel. The following discussion is based on the evolutions of the fuel central temperature, the fuel-cladding gap size and the fuel restructuring (inner void, columnar grain radius) of the HEDL P-19–27 pin as predicted by the TRANSURANUS fuel performance code [16,21], version v1m5j20 [78]. The corresponding experimental data are also included in Figs. 8 and 9 and compared with the results for U-Pu MOX fuel from [19].

The impact of the 5 at.% Am content in the HEDL P-19 fuel on the fuel central temperature is shown in Fig. 7, including also the

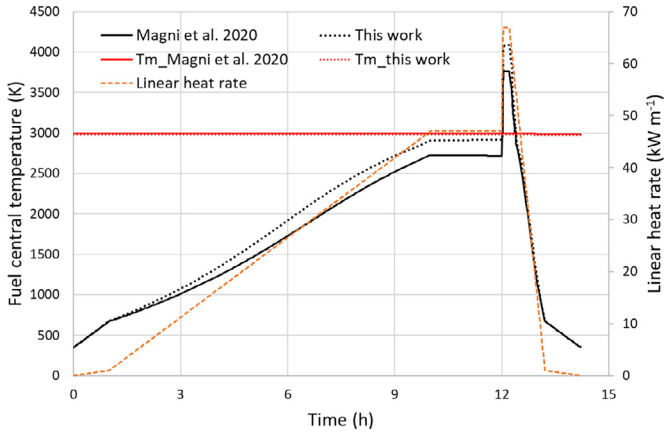

Fig. 7. Evolution in time of the fuel central temperature (black lines) and fuel melting temperatures (red lines), as predicted by TRANSURANUS for the reference HEDL P-19 U-Pu MOX fuel (full lines) or for the hypothetical Am-MOX fuel (dotted lines). The linear heat rate history (dashed orange line) is also included on the secondary axis [20] (For interpretation of the references to color in this figure legend, the reader is referred to the web version of this article). .

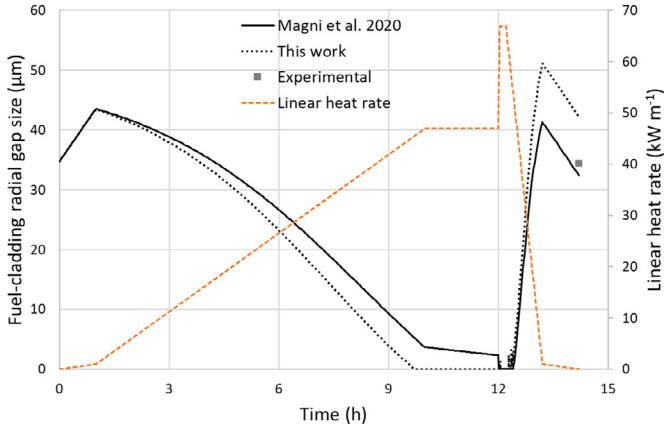

Fig. 8. Evolution in time of the fuel-cladding radial gap size (black lines), as predicted by TRANSURANUS for the reference HEDL P-19 U-Pu MOX fuel (full lines) or for the hypothetical Am-MOX fuel (dotted lines). The experimental value measured on the U-Pu MOX fuel at the end of irradiation is also reported (grey square point). The linear heat rate history (dashed orange line) is included on the secondary axis [20] (For interpretation of the references to color in this figure legend, the reader is referred to the web version of this article). .

linear heat rate evolution bringing the fuel to melting, i.e., a first slower power ramp followed by a fast ramp up to full power, before power shutdown [20]. For both the reference U-Pu MOX fuel and the hypothetical Am-MOX fuel, the central temperature progressively increases during the first slower power rise, reaching a value close to fuel melting already in the power holding phase between 10 and 12 h of irradiation in the Am-MOX case. The fast power ramp brings both kinds of fuels to melting, albeit with a wider radial extent in the Am-MOX pellet (~ 30% instead of ~ 25% of the pellet area, around the centreline) as a consequence of the higher temperatures reached (~ 4000 K instead of ~ 3700 K). The different behaviour in terms of fuel central temperature affects not only the fuel melting, but also the fuel thermal expansion (Fig. 8) and the restructuring (Fig. 9) and is mostly ascribable to the impact of the 5 at.% Am content on the fuel thermal conductivity rather than on the melting temperature. Indeed, as represented by Fig. 7, the fuel melting temperature predicted by the correlation proposed in this work at 5 at.% Am content is only ~ 20 K lower with respect to that of U-Pu MOX (i.e., 2977 K instead of 2994 K), consistent with the limited impact of homogeneous minor

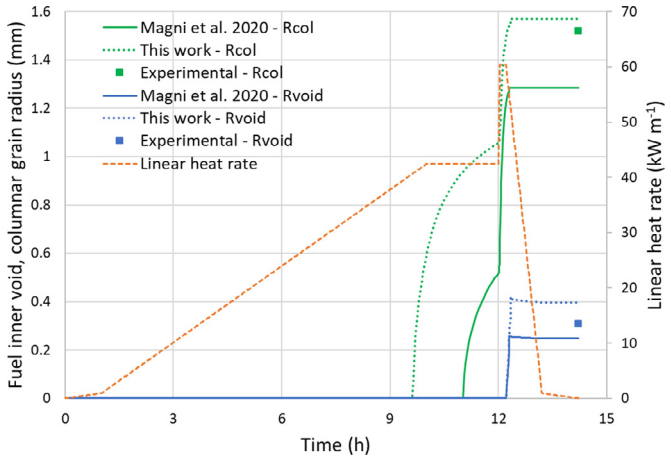

Fig. 9. Evolution in time of the fuel inner void radius (blue lines) and columnar grain radius (green lines), as predicted by TRANSURANUS for the reference HEDL P-19 U-Pu MOX fuel (full lines) or for the hypothetical Am-MOX fuel (dotted lines). The experimental data measured on the U-Pu MOX fuel at the end of irradiation are also reported (blue and green square points, respectively). The linear heat rate history (dashed orange line) is included on the secondary axis [20] (For interpretation of the references to color in this figure legend, the reader is referred to the web version of this article). .

actinides on the melting temperature reported in the current literature [22,31]. As a consequence of the higher fuel centreline temperature, the inception of melting in the Am-MOX is anticipated, reflecting in a lower power-to-melt predicted by TRANSURANUS, i.e., ~ 51.4 kW m^{-1} instead of 57.3 kW m^{-1} for the U-Pu MOX fuel. This confirms the satisfactory accuracy of the code predictions [19] when comparing with the experimental value of 61.7 kW m^{-1}, considering the experimental uncertainty of 6% on the power-to-melt measurements [20].

Considering the fuel-cladding gap size evolution during the HEDL P-19–27 test (Fig. 8), the gap reaches an anticipated closure in case of the hypothetical Am-MOX fuel, already at the end of the first slower ramp, consistently with the higher fuel temperature causing a stronger fuel thermal expansion. The fuel swelling contribution, also enhanced by the fuel temperatures, is deemed of secondary importance given the short irradiation histories performed during the HEDL P-19 campaign. After the gap closure, which occurs also for the experimental U-Pu MOX-fuelled pin during the fast power ramp, the dynamics of gap re-opening during power shutdown proves different between the two simulation cases, leading to different final gap size values at the end of irradiation. The reason for a wider gap re-opening after power shutdown for the Am-MOX pin is attributed to a higher creep due to the longer fuel-cladding mechanical interaction during gap closure, leading to a higher cladding plastic strain (effective plastic strain of ~ 0.7% instead of ~ 0.45%). The agreement between the TRANSURANUS prediction and the measured gap width for the U-Pu MOX fuel at the end of irradiation is remarkable, as shown by Fig. 8.

The higher extent of fuel restructuring in the case of the hypothetical Am-MOX fuel under the HEDL P-19 irradiation conditions (Fig. 9) is the consequence of the higher fuel temperature. The predicted dynamics are similar for the two types of fuel, with an anticipated start of columnar grain growth in the Am-MOX case. Both inner void and columnar grain extensions are enhanced by the fast power ramp. In terms of comparison with the available experimental data at the end of irradiation, the TRANSURANUS predictions seem somewhat conservative, since underestimating the fuel restructuring and hence the beneficial thermal feedback on the fuel temperature regime. Definitive conclusions about this effect would require more and suitable data to compare with.

Conclusions

The aim of this work was to derive and assess novel, physically grounded and comprehensive correlations for the thermal conductivity and melting temperature of minor actinide-bearing mixed-oxide fuels (MA-MOX. i.e., (U, Pu, Am, Np)O_{2-x}). The novel models are based on an extensive review of the currently available literature about data and existing correlations, performed in Sections 2 and 3, respectively, and are developed by extending corresponding correlations for U-Pu MOX fuels, previously published by the same authors, with the inclusion of the Am and Np content effects. The functional form of the herein proposed correlations has been statistically assessed through a p-value analysis on the regressors, which confirmed the inclusion of the comprehensive set of dependencies in both models. The available data, both experimental and from molecular dynamics calculations, allowed the extension of the ranges of applicability of the correlations up to significant Am and Np contents (10 at.% and 12 at.%, respectively) and to high fuel burn-up (150 GWd/t_{HM}). Nevertheless, the minor actinide content effect on the thermal properties of mixed-oxides proves to be limited, at least in the aforementioned ranges where data are currently available. The predictions obtained from the novel MA-MOX correlations are remarkable since within the experimental uncertainties with respect to the data, and the average deviations are in line with or lower than the error of the existing literature correlations. This proves the quality of the approach followed and of the modelling results obtained, able to coherently represent important processes occurring in oxide fuels under irradiation, e.g., the pollution and saturation of the material lattice with fission products as fuel burn-up evolves.

This work represents an advancement with respect to the state-of-the-art modelling implemented in fuel performance codes from the thermal properties point of view, pivotal in determining the fuel temperature regime according to the actual fuel composition and burn-up, and hence the compliance with the margin-to-melting safety limit. In particular, this paper contributes to the analysis of the behaviour of minor actinide-bearing oxide fuels under irradiation, which is recognized as a topic of current interest in view of americium and neptunium burning and transmutation in fast reactors and Generation IV systems. Future developments of the herein presented work could concern first the further assessment, validation and possible refinement of the thermal conductivity and melting temperature correlations proposed, as soon as additional experimental data will become available. This will help to better assess the impact of the minor actinide contents on the fuel thermal properties, currently identified as limited. Moreover, the effects of large deviations from fuel stoichiometry (> 0.05) and high plutonium contents (> 50 at.%) are still to be deeply analysed and understood. In this perspective, molecular dynamics simulations could be exploited to complement the experimental measurements, since MD techniques are currently able to simulate mixed-oxide materials with potentially any composition (e.g., heterogeneous MA-MOX with > 10 at.% MA content) and micro-structural features (also in the hyper-stoichiometry range), hence further extending the ranges of applicability of the present correlations. Nevertheless, the authors suggest first further analyses of the molecular dynamics results before their integration with experimental data, in light of some controversial outcomes of current MD calculations compared to the accepted literature, e.g., an increased melting temperature for slightly hypo-stoichiometric MOX fuel. Moreover, the systematic underestimation of the MD-calculated thermal conductivity data at low temperatures (Fig. 3) could suggest an effect related to the selection of the interatomic potential applied in the MD simulations, which is still an open issue to be investigated.

Additional experimental data and investigations would also be useful on high-porosity MOX and MA-MOX ($> 10\%$ TD), of concern for the un-restructured fuel region or considering the strong porosity migration and accumulation near the pellet centreline in fast reactor fuels and Generation IV conditions. In this way, the current modelling of thermal conductivity valid up to 10% TD could be refined and extended, improving the large deviations obtained from the state-of-the-art data beyond the current range of applicability in terms of fuel porosity. Instead, the impact of the minor actinide concentrations in oxide nuclear fuels could be assessed also via grain-scale simulations, in a more mechanistic way exploiting e.g., the MFPR-F and SCIANTIX codes [79–81]. Among their capabilities, these tools allow evaluating the density of lattice defects induced by fuel self-irradiation (caused mainly by the α-activity of americium) and the fuel lattice recovery by annealing of lattice defects at high temperatures. In addition, the impact on the thermal properties of the concentration of fission products retained in the fuel, evolving during irradiation and sensibly influenced by the high temperatures of fast reactor fuels that promote fission product release, could be accounted for. The use of MFPR-F or SCIANTIX tools could enable a more accurate consideration of the high temperature effects of recovering part of the burn-up degradation of thermal conductivity and melting temperature of oxide nuclear fuels, especially at high burn-up [82]. This would result in the introduction of a sort of effective burn-up, as recently performed in [83] for the modelling of the High Burn-up Structure. The behaviour of thermal conductivity and melting temperature of MOX and MA-MOX fuels at high burn-up indeed requires further investigations, given the current scarcity of experimental data and the current limitations of MD simulations in this respect.

Lastly, a more extensive integral validation of the fuel performance code capabilities towards MA-MOX fuels under irradiation is needed, besides a deep separate-effect validation of the novel correlations for the MA-MOX thermal properties. The applicative example, herein presented to showcase the potential effect of an americium content in MOX fuels concerning the fuel melting and restructuring behaviour in beginning-of-life conditions, should be complemented by further analyses and simulations of the behaviour at extended burn-up of pins employing MA-MOX fuel pellets. Indeed, the proposed thermal conductivity correlation is the first in literature featuring a burn-up dependence for MA-MOX, reasonably based on the U-Pu MOX behaviour [19] (while an existing correlation not accounting for the burn-up effect [22] has been already tested in predicting the thermal performance of short-irradiated Am-MOX pins in the Joyo reactor [54]). Also, the integral impact of a heterogeneous Am content (> 10 at.%) is of interest to assess the feasibility of high-MA content fuel irradiation in fast reactors for enhanced burning and transmutation applications, and will be investigated in the framework of the PATRICIA H2020 European Project [11] once more experimental data will become available for modelling extension and validation purposes.

The identified development paths all fall within the scope of continuously enhancing the predictive capabilities of fuel performance codes towards properties and phenomena peculiar of MOX and MA-MOX fuels under irradiation in fast and Generation IV conditions.

Declaration of Competing Interest

None.

Acknowledgments

This work has received funding from the Euratom research and training programme 2014–2018 through the INSPYRE project under grant agreement No 754329.

Credit authorship contribution statement

Alessio Magni: Conceptualization, Methodology, Acquisition of data, Software, Verification and Validation, Writing – Original Draft, Writing – Review & Editing, Visualization.

Lelio Luzzi: Conceptualization, Writing – Review & Editing, Supervision.

Davide Pizzocri: Methodology, Writing – Review & Editing, Visualization.

Arndt Schubert: Writing – Review & Editing, Visualization.

Paul Van Uffelen: Conceptualization, Methodology, Writing – Review & Editing, Supervision.

Alessandro Del Nevo: Conceptualization, Writing – Review & Editing, Supervision, Funding Acquisition.

References

[1] GIF (Generation IV International Forum), "GIF R&D Outlook for Generation IV Nuclear Energy Systems - 2018 Update", 2018.

[2] GIF (Generation IV International Forum), "Annual Report 2019", 2019. Available: https://www.gen-4.org/gif/jcms/c_44720/annual-reports.

[3] J.-F. Babelot and N. Chauvin, "Joint CEA/JRC Synthesis Report of the Experiment SUPERFACT 1", Report JRC-ITU-TN-99/03, 1999.

[4] E. D'Agata, P.R. Hania, D. Freis, J. Somers, S. Bejaoui, F.F. Charpin, P.J. Baas, R.A.F. Okel, S. van Til, J.M. Lapetite, F. Delage, The MARINE experiment: Irradiation of sphere-pac fuel and pellets of UO_{2-x} for americium breading blanket concept, Nucl. Eng. Des. 311 (2017) 131–141.

[5] A. Gallais-During, F. Delage, S. Bejaoui, S. Lemehov, J. Somers, D. Freis, W. Maschek, S. van Til, E. D'Agata, C. Sabathier, Outcomes of the PELGRIMM project on Am-bearing fuel in pelletized and spherepac forms, J. Nucl. Mater. 512 (2018) 214–226.

[6] EERA-JPNM, "INSPYRE - Investigations Supporting MOX Fuel Licensing in ESNII Prototype Reactors", 2017. [Online]. Available: http://www.eera-jpnm.eu/inspyre/.

[7] A. Magni, P. Van Uffelen, A. Schubert, L. Luzzi, P. Del Prete, A. Del Nevo, "Improved models of thermal conductivity, melting temperature and JOG for MOX fuels with low Minor Actinide contents", INSPYRE Deliverable D6.5, 2021, to be published.

[8] H. Aït Abderrahim, P. Baeten, D. De Bruyn, R. Fernandez, MYRRHA - A multi-purpose fast spectrum research reactor, Energy Convers. Manag. 63 (2012) 4–10.

[9] H. Aït Abderrahim, P. Baeten, A. Sneyers, M. Schyns, P. Schuurmans, A. Kochetkov, G. Van den Eynde, J.-L. Biarrotte, Partitioning and transmutation contribution of MYRRHA to an EU strategy for HLW management and main achievements of MYRRHA related FP7 and H2020 projects: MYRTE, MARISA, MAXSIMA, SEARCH, MAX, FREYA, ARCAS, Nucl. Sci. Technol. 33 (2020) 1–8.

[10] V. Sobolev, S. Lemehov, N. Messaoudi, P. Van Uffelen, H. Aït Abderrahim, Modelling the behaviour of oxide fuels containing minor actinides with urania, thoria and zirconia matrices in an accelerator-driven system, J. Nucl. Mater. 319 (2003) 131–141.

[11] European Union's Horizon 2020 Research and Innovation programme, "PATRICIA - Partitioning And Transmuter Research Initiative in a Collaborative Innovation Action", 2020. [Online]. Available: https://patricia-h2020.eu/.

[12] GIF (Generation IV International Forum), "Technology Roadmap Update for Generation IV Nuclear Energy Systems", 2014. Available: https://www.gen-4.org/gif/upload/docs/application/pdf/2014-03/gif-tru2014.pdf.

[13] G. Locatelli, M. Mancini, N. Todeschini, Generation IV nuclear reactors: Current status and future prospects, Energy Policy 61 (2013) 1503–1520.

[14] D. Olander, Nuclear fuels - Present and future, J. Nucl. Mater. 389 (1) (2009) 1–22.

[15] C.O.T. Galvin, P.A. Burr, M.W.D. Cooper, P.C.M. Fossati, R.W. Grimes, Using molecular dynamics to predict the solidus and liquidus of mixed oxides $(Th,U)O_2$, $(Th,Pu)O_2$ and $(Pu,U)O_2$, J. Nucl. Mater. 534 (2020) 152127.

[16] European CommissionTRANSURANUS Handbook, Joint Research Centre, Karlsruhe, Germany, 2020.

[17] K. Lassmann, URANUS - A computer programme for the thermal and mechanical analysis of the fuel rods in a nuclear reactor, Nucl. Eng. Des. 45 (1978) 325–342.

[18] K. Lassmann, TRANSURANUS: a fuel rod analysis code ready for use, J. Nucl. Mater. 188 (1992) 295–302 no. C.

[19] A. Magni, T. Barani, A. Del Nevo, D. Pizzocri, D. Staicu, P. Van Uffelen, L. Luzzi, Modelling and assessment of thermal conductivity and melting behaviour of MOX fuel for fast reactor applications, J. Nucl. Mater. 541 (2020) 152410.

[20] R.B. Baker, Integral Heat Rate-to-incipient Melting in UO_2-PuO_2 Fast Reactor Fuel, Report HEDL-TME 77-23 (1978).

[21] A. Magni, A. Del Nevo, L. Luzzi, D. Rozzia, M. Adorni, A. Schubert, P. Van Uffelen, The TRANSURANUS fuel performance code, in: J. Wang, X. Li, C. Allison, J. Hohorst (Eds.), Nuclear Power Plant Design and Analysis Codes - Development, Validation and Application, Elsevier, 2021, pp. 161–205. Chap. 8, Woodhead Publishing Series in Energy.

[22] M. Kato, K. Maeda, T. Ozawa, M. Kashimura, Y. Kihara, Physical properties and irradiation behavior analysis of Np- and Am-Bearing MOX Fuels, J. Nucl. Sci. Technol. 48 (4) (2011) 646–653.

[23] D. Prieur, R.C. Belin, D. Manara, D. Staicu, J.C. Richaud, J.F. Vigier, A.C. Scheinost, J. Somers, P. Martin, Linear thermal expansion, thermal diffusivity and melting temperature of Am-MOX and Np-MOX, J. Alloys Compd. 637 (2015) 326–331.

[24] K. Morimoto, M. Kato, M. Ogasawara, M. Kashimura, T. Abe, Thermal conductivities of (U, Pu, Am)O_2 solid solutions, J. Alloys Compd. 452 (1) (2008) 54–60.

[25] K. Morimoto, M. Kato, M. Ogasawara, M. Kashimura, Thermal conductivities of hypostoichiometric (U, Pu, Am)O_{2-x} oxide, J. Nucl. Mater. 374 (3) (2008) 378–385.

[26] K. Morimoto, M. Kato, M. Ogasawara, M. Kashimura, Thermal conductivity of $(U,Pu,Np)O_2$ solid solutions, J. Nucl. Mater. 389 (1) (2009) 179–185.

[27] K. Kurosaki, J. Adachi, M. Katayama, M. Osaka, K. Tanaka, M. Uno, S. Yamanaka, Molecular dynamics studies of americium-containing mixed oxide fuels, J. Nucl. Sci. Technol. 43 (10) (2006) 1224–1227.

[28] W. Li, J. Ma, J. Du, G. Jiang, Molecular dynamics study of thermal conductivities of $(U_{0.7-x}Pu_{0.3}Am_x)O_2$, J. Nucl. Mater. 480 (2016) 47–51.

[29] J.-M. Bonnerot, "Propriétés thermiques des oxydes mixtes d'uranium et de plutonium", PhD thesis, Rapport CEA-R-5450, 1988.

[30] A. Magni, L. Luzzi, P. Van Uffelen, D. Staicu, P. Console Camprini, P. Del Prete, A. Del Nevo, "Report on the improved models of melting temperature and thermal conductivity for MOX fuels and JOG", INSPYRE Deliverable D6.2, version 2, 2020.

[31] K. Konno, T. Hirosawa, Melting temperature of irradiated fast reactor mixed oxide fuels, J. Nucl. Sci. Technol. 35 (7) (1998) 494–501.

[32] M. Kato, K. Morimoto, H. Sugata, K. Konashi, M. Kashimura, T. Abe, Solidus and liquidus temperatures in the UO_2-PuO_2 system, J. Nucl. Mater. 373 (1–3) (2008) 237–245, doi:10.1016/j.jnucmat.2007.06.002.

[33] K. Konno, T. Hirosawa, Melting temperature of mixed oxide fuels for fast reactors, J. Nucl. Sci. Technol. 39 (7) (2002) 771–777.

[34] K. Tanaka, M. Osaka, S. Miwa, T. Hirosawa, K. Kurosaki, H. Muta, M. Uno, S. Yamanaka, Preparation and characterization of the simulated burnup americium-containing uranium-plutonium mixed oxide fuel, J. Nucl. Mater. 420 (1–3) (2012) 207–212.

[35] M. Kato, K. Morimoto, H. Sugata, K. Konashi, M. Kashimura, T. Abe, Solidus and liquidus of plutonium and uranium mixed oxide, J. Alloys Compd. 452 (1) (2008) 48–53.

[36] R. Böhler, M.J. Welland, D. Prieur, P. Cakir, T. Vitova, T. Pruessmann, I. Pidchenko, C. Hennig, C. Guéneau, R.J.M. Konings, D. Manara, Recent advances in the study of the UO_2-PuO_2 phase diagram at high temperatures, J. Nucl. Mater. 448 (1–3) (2014) 330–339.

[37] M. Strach, D. Manara, R.C. Belin, J. Rogez, Melting behavior of mixed U-Pu oxides under oxidizing conditions, Nucl. Instruments Methods Phys. Res. Sect. B Beam Interact. with Mater. Atoms 374 (2016) 125–128.

[38] C. Guéneau, P. Fouquet-Métivier, P. Martin, R. Vauchy, M. Freyss, M.S. Talla Noutack, I. Cheik Njifon, Thermodynamic modelling of the (U-Pu-Am-O) system, INSPYRE Deliverable D1.1 (2019) D1.1.

[39] P. Fouquet-Métivier, L. Medyk, R. Vauchy, P.M. Martin, L. Vlahovic, D. Robba, C. Guéneau, Melting behaviour of $(U,Pu)O_2$ SFRs fuels: influence of Pu and Am contents and oxygen stoichiometry, in: NuMat 2020: The Nuclear Materials Conference, Elsevier, 2020, p. 2020. 26-29 October, online.

[40] K. Morimoto, M. Kato, H. Uno, A. Hanari, T. Tamura, H. Sugata, T. Sunaoshi, S. Kono, Preparation and characterization of (Pu, U, Np, Am, simulated FP)O_{2-x}, J. Phys. Chem. Solids vol. 66 (2–4) (2005) 634–638.

[41] Y. Ida, Interionic repulsive force and compressibility of ions, Phys. Earth Planet. Inter. 13 (2) (1976) 97–104.

[42] K. Maeda, S. Sasaki, M. Kato, Y. Kihara, Behavior of Si impurity in Np-Am-MOX fuel irradiated in the experimental fast reactor Joyo, J. Nucl. Mater. 385 (1) (2009) 178–183.

[43] K. Maeda, S. Sasaki, M. Kato, Y. Kihara, Short-term irradiation behavior of minor actinide doped uranium plutonium mixed oxide fuels irradiated in an experimental fast reactor, J. Nucl. Mater. 385 (2) (2009) 413–418.

[44] K. Maeda, S. Sasaki, M. Kato, Y. Kihara, Radial redistribution of actinides in irradiated FR-MOX fuels, J. Nucl. Mater. 389 (1) (2009) 78–84.

[45] K. Maeda, K. Katsuyama, Y. Ikusawa, S. Maeda, Short-term irradiation behavior of low-density americium-doped uranium-plutonium mixed oxide fuels irradiated in a fast reactor, J. Nucl. Mater. 416 (1–2) (2011) 158–165.

[46] K. Yokohama, M. Watanabe, M. Kato, D. Tokoro, M. Sugimoto, Thermal conductivity measurement of high Am bearing mixed oxide fuel, in: NuMat 2020: The Nuclear Materials Conference, Elsevier, 2020, p. 2020. 26-29 October, online.

[47] C. Cozzo, D. Staicu, J. Somers, A. Fernandez, R.J.M. Konings, Thermal diffusivity and conductivity of thorium-plutonium mixed oxides, J. Nucl. Mater. 416 (1–2) (2011) 135–141.

[48] M. Saoudi, D. Staicu, J. Mouris, A. Bergeron, H. Hamilton, M. Naji, D. Freis, M. Cologna, Thermal diffusivity and conductivity of thorium-uranium mixed oxides, J. Nucl. Mater. 500 (2018) 381–388.

[49] D. Jain, C.G.S. Pillai, B.S. Rao, R.V. Kulkarni, E. Ramdasan, K.C. Sahoo, Thermal diffusivity and thermal conductivity of thoria-lanthana solid solutions up to 10 mol.% $LaO_{1.5}$, J. Nucl. Mater. 353 (1–2) (2006) 35–41.

[50] K. Morimoto, M. Kato, A. Komeno, M. Kashimura, Evaluation of thermal conductivity of $(U,Pu,Am)O_{2-x}$, Trans. Am. Nucl. Soc. 97 (2007) 618–619.

[51] J. Fink, Thermophysical properties of uranium dioxide, J. Nucl. Mater. 279 (1) (2000) 1–18.

[52] J.J. Carbajo, G.L. Yoder, S.G. Popov, V.K. Ivanov, A review of the thermophysical properties of MOX and UO_2 fuels, J. Nucl. Mater. 299 (3) (2001) 181–198.

[53] Y. Ikusawa, K. Morimoto, M. Kato, K. Saito, M. Uno, The Effects of Plutonium Content and Self-Irradiation on Thermal Conductivity of Mixed Oxide Fuel, Nucl. Technol. 205 (3) (2019) 474–485.
[54] T. Ozawa, S. Hirooka, M. Kato, S. Novascone, P. Medvedev, Development of fuel performance analysis code BISON for MOX, named Okami: Analyses of pore migration behavior to affect the MA-bearing MOX fuel restructuring, J. Nucl. Mater. 553 (2021) 153038.
[55] Y. Ikusawa, T. Ozawa, S. Hirooka, K. Maeda, M. Kato, S. Maeda, Development and verification of the thermal behaviour analysis code for MA containing MOX fuel, in: Proceedings of the 22nd International Conference on Nuclear Engineering ICONE22, 7-11 July 2014, Prague, Czech Republic, pp. 1–6, 2014.
[56] D. Bathellier, M. Lainet, M. Freyss, P. Olsson, E. Bourasseau, A new heat capacity law for UO_2, PuO_2 and (U,Pu)O_2 derived from molecular dynamics simulations and useable in fuel performance codes, J. Nucl. Mater. 549 (2021) 152877.
[57] MathWorks, "MATLAB code", 2019. [Online]. Available: https://uk.mathworks.com/products/matlab.html.
[58] The R Foundation, "R version 3.5.1″, 2018. [Online]. Available: https://www.r-project.org/.
[59] S. Lemehov, V. Sobolev, P. Van Uffelen, Modelling thermal conductivity and self-irradiation effects in mixed oxide fuels, J. Nucl. Mater. 320 (1–2) (2003) 66–76.
[60] M.W.D. Cooper, S.C. Middleburgh, R.W. Grimes, Modelling the thermal conductivity of $(U_xTh_{1-x})O_2$ and $(U_xPu_{1-x})O_2$, J. Nucl. Mater. 466 (2015) 29–35.
[61] K. Yamamoto, T. Hirosawa, K. Yoshikawa, K. Morozumi, S. Nomura, Melting temperature and thermal conductivity of irradiated mixed oxide fuel, J. Nucl. Mater. 204 (1993) 85–92 no. C.
[62] D. Staicu, E. Dahms, T. Wiss, O. Benes, J. Colle, Preparing ESNII for HORIZON 2020 - Deliverable D7.4.2 - Properties measurements on irradiated fuels (NESTOR 3), ESNII+ Deliverable D7.4.2 (2017) D7.4.2.
[63] D. Staicu, E. Dahms, D. Manara, J.-Y. Colle, O. Benes, M. Marchetti, D. Robba, N. Chauvin, P.M. Martin, Preparing ESNII for HORIZON 2020 - Deliverable D7.4.1 - Measurement of properties of fresh Phenix fuel, ESNII+ Deliverable D7.4.1, 2017.
[64] D. Staicu, E. Dahms, D. Manara, M. Marchetti, D. Robba, T. Wiss, B. Cremer, O. Dieste-Bianco, N. Chauvin, P.M. Martin, Preparing ESNII for HORIZON 2020 - Deliverable D7.3.4 - Characterization and measurement of properties of fresh TRABANT fuel, ESNII+ Deliverable D7.3.4, 2017.
[65] D. Staicu, M. Barker, Thermal conductivity of heterogeneous LWR MOX fuels, J. Nucl. Mater. 442 (1–3) (2013) 46–52.
[66] H. Matzke, Diffusion processes and surface effects in non-stoichiometric nuclear fuel oxides UO_{2+x} and (U, Pu)$O_{2\pm x}$, J. Nucl. Mater. 114 (2–3) (1983) 121–135.
[67] P. Pernot, F. Cailliez, A critical review of statistical calibration/prediction models handling data inconsistency and model inadequacy, AIChE J 63 (10) (2017) 4642–4665.
[68] T. Tachibana, T. Ohmori, S. Yamanouchi, T. Itaki, Determination of melting point of mixed-oxide fuel irradiated in fast breeder reactor, J. Nucl. Sci. Technol. 22 (2) (1985) 155–157.
[69] L.J. Siefken, E.W. Coryel, E.A. Harvego, J.K. Hohorst, SCDAP/RELAP5/MOD 3.3 Code Manual, MATPRO - A Library of Materials Properties for Light-Water-Reactor Accident Analysis 4 (2001).
[70] D. Manara, C. Ronchi, M. Sheindlin, M. Lewis, M. Brykin, Melting of stoichiometric and hyperstoichiometric uranium dioxide, J. Nucl. Mater. 342 (1–3) (2005) 148–163.
[71] P.M. Martin, N. Chauvin, J.-P. Ottaviani, D. Staicu, R. Calabrese, N. Vér, G. Trillon, J. Klousal, A. Fedorov, M.A. Mignanelli, S. Portier, M. Verwerft, Preparing ESNII for HORIZON 2020 - Deliverable D7.5.1 - Catalog on MOX properties for fast reactors, ESNII+ Deliverable D7.5.1, 2017.
[72] F. De Bruycker, K. Boboridis, R.J.M. Konings, M. Rini, R. Eloirdi, C. Guéneau, N. Dupin, D. Manara, On the melting behaviour of uranium/plutonium mixed dioxides with high-Pu content: A laser heating study, J. Nucl. Mater. 419 (1–3) (2011) 186–193.
[73] T. Hirosawa, I. Sato, Burnup dependence of melting temperature of FBR mixed oxide fuels irradiated to high burnup, J. Nucl. Mater. 418 (1–3) (2011) 207–214.
[74] C.T. Walker, Assessment of the radial extent and completion of recrystallisation in high burn-up UO_2 nuclear fuel by EPMA, J. Nucl. Mater. 275 (1) (1999) 56–62.
[75] J. Noirot, L. Desgranges, J. Lamontagne, Detailed characterization of high burn-up structures in oxide fuels, J. Nucl. Mater. 372 (2–3) (2008) 318–339.
[76] F. Lemoine, D. Baron, P. Blanpain, Key parameters for the High Burnup Structure formation thresholds, in: Proceedings of 2010 LWR Fuel Performance / TopFuel / WRFPM2010, American Nuclear Society, 29 September 2010, p. 26. Orlando, Florida, USA, 2010.
[77] M.G. Adamson, E.A. Aitken, R.W. Caputi, Experimental and thermodynamic evaluation of the melting behavior of irradiated oxide fuels, J. Nucl. Mater. 130 (1985) 349–365 C.
[78] P. Van Uffelen, A. Schubert, L. Luzzi, T. Barani, A. Magni, D. Pizzocri, M. Lainet, V. Marelle, B. Michel, B. Boer, S. Lemehov, A. Del Nevo, Incorporation and verification of models and properties in fuel performance codes, INSPYRE Deliverable D7.2, 2020.
[79] D. Pizzocri, T. Barani, L. Luzzi, SCIANTIX: A new open source multi-scale code for fission gas behaviour modelling designed for nuclear fuel performance codes, J. Nucl. Mater. 532 (2020) 152042.
[80] D. Pizzocri, T. Barani, L. Luzzi, "SCIANTIX code", 2018. [Online]. Available: https://gitlab.com/poliminrg/sciantix.
[81] T.R. Pavlov, F. Kremer, R. Dubourg, A. Schubert, P. Van Uffelen, Towards a More Detailed Mesoscale Fission Product Analysis in Fuel Performance Codes: a Coupling of the TRANSURANUS and MFPR-F Codes, TopFuel2018 - Reactor Fuel Performance, 30 September - 4 October 2018, Prague, Czech Republic, 2018.
[82] D. Staicu, V.V. Rondinella, C.T. Walker, D. Papaioannou, R.J.M. Konings, C. Ronchi, M. Sheindlin, A. Sasahara, T. Sonoda, M. Kinoshita, Effect of burn-up on the thermal conductivity of uranium-gadolinium dioxide up to 100 GWd/tHM, J. Nucl. Mater. 453 (1–3) (2014) 259–268.
[83] T. Barani, D. Pizzocri, F. Cappia, L. Luzzi, G. Pastore, P. Van Uffelen, Modeling high burnup structure in oxide fuels for application to fuel performance codes. Part I: High burnup structure formation, J. Nucl. Mater. 539 (2020) 152296.